ANALYSIS OF PARTIAL DISCHARGE SIGNALS USING DIGITAL SIGNAL PROCESSING TECHNIQUES

A Thesis Submitted in Partial Fulfillment

of the Requirements for the Award of the Degree of

Master of Technology

in

Power Control & Drives

By

ALOK KUMAR PRADHAN

Roll No. 210EE2107

Department of Electrical Engineering

National Institute of Technology

Rourkela-769008

May, 2012

ANALYSIS OF PARTIAL DISCHARGE SIGNALS USING DIGITAL SIGNAL PROCESSING TECHNIQUES

A Thesis Submitted in Partial Fulfillment

of the Requirements for the Award of the Degree of

Master of Technology

in

Power Control & Drives

By

ALOK KUMAR PRADHAN

Under the Guidance of

Prof. Subrata Karmakar

Department of Electrical Engineering

National Institute of Technology

Rourkela-769008

May, 2012

National Institute of Technology

Rourkela

CERTIFICATE

This is to certify that the thesis entitled, "**Analysis of Partial Discharge Signals using Digital Signal Processing Techniques**" submitted by **Alok Kumar Pradhan (Roll No. 210EE2107)** in partial fulfillment of the requirements for the award of Master of Technology Degree in Electrical Engineering with specialization in Power Control & Drives during 2011 - 2012 at the National Institute of Technology, Rourkela is an authentic work carried out by him under my supervision and guidance.

To the best of my knowledge, the matter embodied in the thesis has not been submitted to any other University / Institute for the award of any Degree or Diploma.

Date

Prof. S. Karmakar
Department of Electrical Engineering
National Institute of Technology
Rourkela-769008

Acknowledgement

I am thankful to many people who contributed through their support, knowledge and friendship, to this work.

I am grateful to my guide Prof. S. Karmakar for giving me the opportunity to work on this area with vast opportunities. His valuable guidance made me learn some of the advanced concepts during my work. I sincerely appreciate the freedom Prof. S. Karmakar provided me to explore new ideas in the field of my work. He supported and encouraged me throughout the project work.

I would like to express my gratitude to Prof. A. K. Panda, Prof. B. D. Subudhi and Prof. (Mrs.) Susmita Das for their valuable suggestions that helped me improve my research work.

My hearty thanks to all my friends for being with me during this work. I render my respect to all my family members for giving me mental support and inspiration for carrying out my research work.

Alok Kumar Pradhan

Contents

Abstract

Partial discharge (PD) measurements have emerged as a powerful diagnostic tool for condition monitoring of insulation in high voltage equipments. Study of PD patterns reveals the nature and severity of the defects present in the insulation. Nowadays online and onsite PD measurements are preferred to keep the equipment in service while assessing its condition. A major difficulty in such measurements is to extract the PD signal from severe noise and interferences. Various time and frequency domain de-noising techniques are adopted for the extraction of PD signal. Recent research shows that wavelet analysis is a powerful tool in de-noising PD signals. Wavelet analysis can be performed using discrete wavelet transform (DWT) and second generation wavelet transform (SGWT) (also called lifting wavelet transform). In the wavelet analysis based de-noising of PD signals, selection of mother wavelet, maximum decomposition level, and thresholding rule are some of the important issues that affect the de-noising results. Further, time-frequency analysis of PD signal can be performed using S-transform. S-transform is an effective tool for the time-frequency analysis of a signal. This work applies different wavelet based de-noising techniques to five noisy PD signals having different characteristics. Among the five signals four signals are numerically simulated and one is a practical signal. The signals are de-noised using DWT and SGWT based de-noising schemes. The de-noising schemes adopt different types of mother wavelet selection methods, and thresholding rules. Based on the de-noising techniques, varied de-noising results are obtained. A comparative analysis of the de-noising results is made using various de-noising performance indices. Then the time-frequency analysis of the de-noised practical signal is made using S-transform. From the results of the work it emerges that wavelet analysis is a superior tool for the extraction of PD signals. And selection of mother wavelet and thresholding rule for the wavelet based de-noising, depends on the type of signal and the severity of noise and interferences.

List of Figures

List of Tables

List of Abbreviations

AE	Amplitude Error
CWT	Continuous Wavelet Transform
DEP	Damped Exponential Pulse
DOP	Damped Oscillatory Pulse
DSI	Discrete Spectral Interference
DWT	Discrete Wavelet Transform
EBWS	Energy Based Wavelet Selection
FT	Fourier Transform
HV	High Voltage
INR	Interference to Noise Ratio
LS	Lifting Scheme
LWT	Lifting Wavelet Transform
MSD	Multi-Resolution Signal Decomposition
MSE	Mean Square Error
PD	Partial Discharge
QMF	Quadrature Mirror Filter
RNL	Reduction in Noise Level
SGWT	Second Generation Wavelet Transform
SNR	Signal to Noise Ratio
STFT	Short-Time Fourier Transform
TFR	Time-Frequency Representation
WGN	White Gaussian Noise
WT	Wavelet Transform

Chapter 1
Introduction

1.1 Introduction

Electrical insulation is an important component of high voltage (HV) power apparatus. In spite of the technological advancements, manufacturing of a perfect insulator has been an ideal concept. In reality the insulators are contaminated with various kinds of impurities. It has been studied that in most cases degradation of insulation is the primary cause of failure of HV apparatus. Failure of the insulation in HV equipments while in service leads to serious health, safety, environmental and economic consequences [1, 2]. Hence, it is necessary to detect the degradation of the insulation earlier, so that remedial measures can be taken. When degradation occurs in insulation, irrespective of the cause, small electrical sparks within the insulation are generated which are called as partial discharge (PD) [2]. Therefore PD measurements have emerged as a powerful diagnostic tool for insulation system condition monitoring. Using PD signal analysis the PD activity can be categorized, and the nature and the severity of the degradation can be studied [2]. Nowadays, computer based PD measurements are performed online and onsite to keep the equipment in service while monitoring it. The difficulty involved in such measurements is that the surrounding noise and interferences corrupt the acquired PD signal, causing trouble in the study of the signal. Hence, it is necessary to extract the PD pulses before further processing. Various time and frequency domain de-noising tools are adopted to extract the PD pulses from severe noise and interferences. Recent research shows that wavelet transform (WT) is a powerful tool in de-noising PD signals. Partial discharge pulses are irregular, transient and non-periodical in nature. As the WT is an effective tool in analyzing the transient, irregular and non-periodical signals in time-scale domain, it is employed to de-noise and analyze the PD signals [3]. Wavelet transform can be adopted in both time and frequency domain. The frequency domain approach adopts convolution of the signal with the impulse response of the wavelet filters, where as time domain approach called lifting wavelet transform employs lifting scheme. Further, the extracted PD signal is analyzed using signal processing tools like Fourier transform (FT), short-time Fourier transform (STFT) and S-transform etc. The FT shows the frequency components of a signal; but fails to show the position of occurrence of

the frequencies. The STFT gives the time-frequency representation of a signal but possesses a constant resolution. Wavelet transform gives the time-scale representation of a signal, which requires interpretation of the scale to frequency domain. S-transform overcomes the above difficulties and gives the time-frequency representation of a signal with varying resolutions.

1.2 Literature survey

Extensive research works have been pursued in the area of application of digital signal processing techniques to partial discharge signals analysis. Ramu and Nagamani [4] explained the various issues related to PD measurements for condition monitoring of HV equipments. They discussed the processes leading to PD and various electrical methods of PD measurements. They mentioned the different kinds of noise and interferences that affect the PD signals during online and onsite measurement. Also they proposed the WT as a tool to de-noise the PD signals. Ma et al. [2] used the characteristics of the detection circuits to simulate two types of PD pulses called damped exponential pulse (DEP) and damped oscillatory pulse (DOP). They used correlation coefficient to find out the suitability of wavelets to be used as mother wavelets for the study of the two pulses. They applied WT for extracting the DEP and DOP pulses immersed in noise. Kim and Aggarwal [5] presented the theory of wavelet transform and its advantages compared to the earlier methods like FT and STFT. They proposed the suitability of WT for transient signal analysis. Satish and Nazneen [1] proposed a wavelet based de-noising method for extracting PD signals from severe noise and interferences. The de-noising method uses reconstructed time domain detail and approximation components to recover the signal in harsh conditions. In the de-noising method the reconstructed components corresponding to the PD signal are kept and others are discarded. They implemented the de-noising scheme on simulated signals corrupted by severe noise and interferences and evaluated the de-noising method using de-noising performance indices. Zhou et al. [3] proposed a method for selecting the optimal mother wavelet for discrete wavelet transform (DWT) based de-noising of PD signal. This method calculates the energy distribution of the signal over all the DWT decomposition levels using various wavelets and selects the wavelet which retains most energy in a single level. They applied the method to a single PD pulse and the nature of the pulse was previously known. Ma et al. [6] proposed a wavelet selection method and an automatic thresholding rule for the wavelet based de-noising of PD signals. The mother wavelet selection method uses cross correlation coefficient and the

thresholding method is based on the median value of the coefficients of a decomposition level. Li et al. [7] proposed a scale dependent wavelet selection method for WT based de-noising. In the proposed scheme a wavelet is selected as optimal mother wavelet if it generates the approximation with maximum energy percentage among all the wavelets considered. The scheme is repeated for each level. Zhang et al. [8] proposed a new thresholding method for wavelet based de-noising of PD signal. The thresholding method decomposes the noise first using DWT and the threshold values for the PD signal de-noising are chosen according to the maximum values of noise coefficients at each level. Song et al. [9] applied second generation wavelet transform for the data de-noising in PD measurement. They applied the method to both simulated and practical data. The de-noising method, also called lifting wavelet transform method is a time domain method in which the wavelet filters can be modified to suit the requirements. For the time-frequency analysis of a PD signal, S-transform can be employed. Stockwell et al. [10] proposed S transform for time frequency representation of a signal. S-transform is an improved version of WT and STFT. Stockwell [11] presented the derivation of S transform and mentioned the procedure to implement it. Mishra et al. [12] presented S transform based probabilistic neural network classifier for recognition of power quality disturbances. They have extracted important information in terms of magnitude phase and frequency from the S-matrix. Sahu et al. [13] proposed a modified Gaussian window based S-transform for the time-frequency analysis of a signal. The proposed scheme improves the time frequency resolution. More work on wavelet analysis and S-transform is found in [14-23].

1.3 Motivation and objective of the work

Extraction of PD signal from severe noise and interferences is the main difficulty in PD measurement. Among the various de-noising methods used for the extraction of PD signals, wavelet transform based de-noising methods are more powerful. Wavelet transform based de-noising of PD signals is performed in different ways. There are different methods for the selection of mother wavelet, determination of maximum decomposition level and thresholding of the coefficients. All the methods have their own advantages and disadvantages. Hence, a comparison between the different wavelet based PD signal de-noising techniques is necessary. Further, the de-noised PD signal is processed through various digital signal processing techniques to analyze the PD characteristics. Recent research shows that for the time-frequency

analysis of a signal, S-transform is an effective tool. It eliminates the drawbacks of STFT and wavelet transform. The objective of this work is

- To numerically simulate noisy PD signals having different characteristics
- To apply different wavelet transform based techniques for de-noising the simulated PD signals and a practical PD signal
- To evaluate the performances of the adopted PD signal de-noising methods
- To analyze the practical PD signal using S-transform

1.4 Thesis layout

Chapter 1 reviews the literature on concept of PD, wavelet based PD signal analysis and S-transform based time frequency analysis.

Chapter 2 describes the mechanism of PD in the insulation of high voltage equipments. It also introduces PD measurement as a method for online condition monitoring of HV equipments. The two types of PD pulses depending on the nature of detection circuits are mentioned and simulated numerically. A practical signal acquired in laboratory is also introduced in the chapter.

Chapter 3 employs DWT based de-noising methods for the extraction of clean PD signal. The theory of DWT is presented first and then the various issues related to the wavelet based de-noising, like optimal mother wavelet selection, selection of maximum decomposition level, and choosing a proper thresholding rule are mentioned. Various de-noising performance indices used to evaluate PD signal de-noising methods are mentioned. The simulated and practical noisy PD signals are de-noised using the DWT, adopting different wavelet selection methods and thresholding rules.

Chapter 4 employs second generation wavelet transform (SGWT) for the de-noising of the PD signals. A comparative study of the DWT and SGWT based de-noising results is made in this chapter.

Chapter 5 employs S transform for the time-frequency representation of the de-noised practical PD signal.

Chapter 6 summarizes the results obtained in various chapters and the scope for future work is discussed in brief.

Chapter 2
Partial Discharge Concept

2.1 Introduction

Insulation is an important component of HV power equipments used to isolate the energized conductors at different potentials and high voltage conductors from ground. Insulation in power equipments may also be used for cooling and internal electrical discharge suppression purposes. The insulation can be in any of the three states of matter. It is always desirable to have perfect insulation in electrical equipments. However the defects present in the insulation degrades the quality of the insulation. Defect in insulation is defined as any unintended material included in the matrix of insulation [4]. The presence of defects lowers the quality of the insulation. The size of defects in insulation is generally in sub-micron level and is negligible as compared to the thickness of the insulation. Some of the examples of defects are air bubbles, voids, micro-cracks, improper contact between insulation and conducting surface, de-laminating of varnish in winding wire etc [4]. The process of manufacturing insulation structure involves several stages starting from selection and preparation of raw materials, processing of raw materials, thermal or chemical treatment if essential etc. The whole process of providing electrical insulation in a power apparatus involves man, materials, machines and different environmental conditions. It is therefore very difficult to achieve a perfect electrical insulation without defects as it may get contaminated during the process of manufacturing. The influence of surrounding thermal, electrical, mechanical and environmental stresses may also cause defects in electrical insulation during its operation. Defects in high voltage power equipments like power-transformers, machines, switchgears, underground cables etc are more critical as they lead to electrical discharges [4].

2.2 Partial discharge in solid insulation

Presence of weaker dielectrics or defects in solid insulation is shown in Fig. 2.1. In Fig. 2.1(a) the expression for capacitances C_a , C_s and the electric fields E_a, E_s with usual notations can be written as [4]:

$$\frac{E_a}{E_s} = \frac{C_a}{C_s} \tag{1}$$

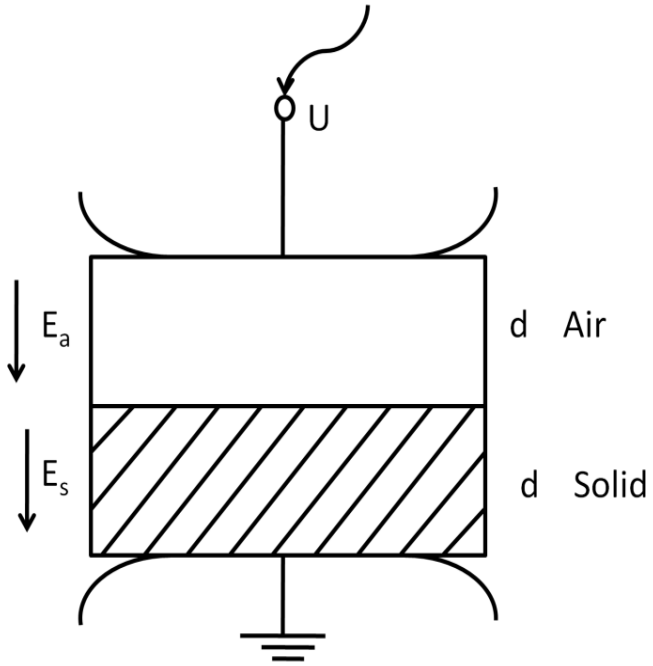

Figure 2.1(a) Air gap and solid insulation.

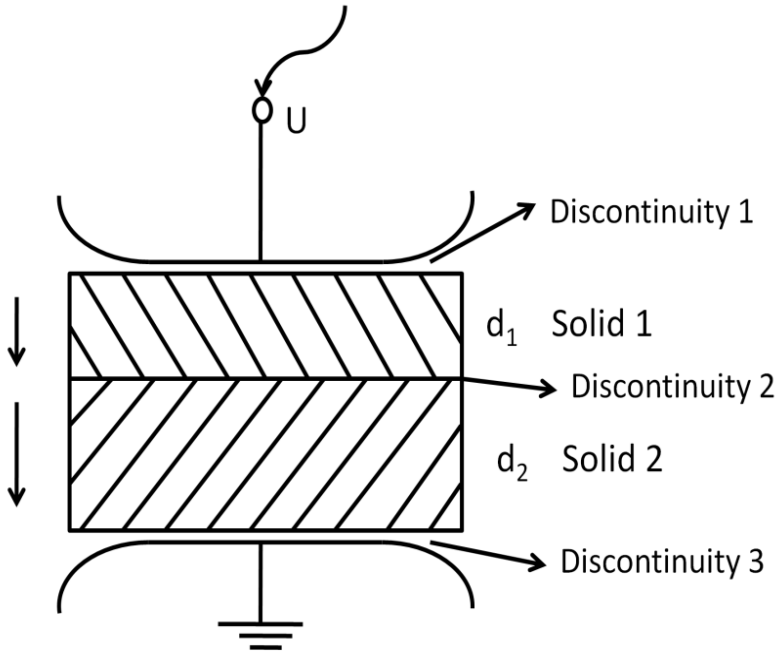

Figure 2.1(b) Two different solid insulation media.

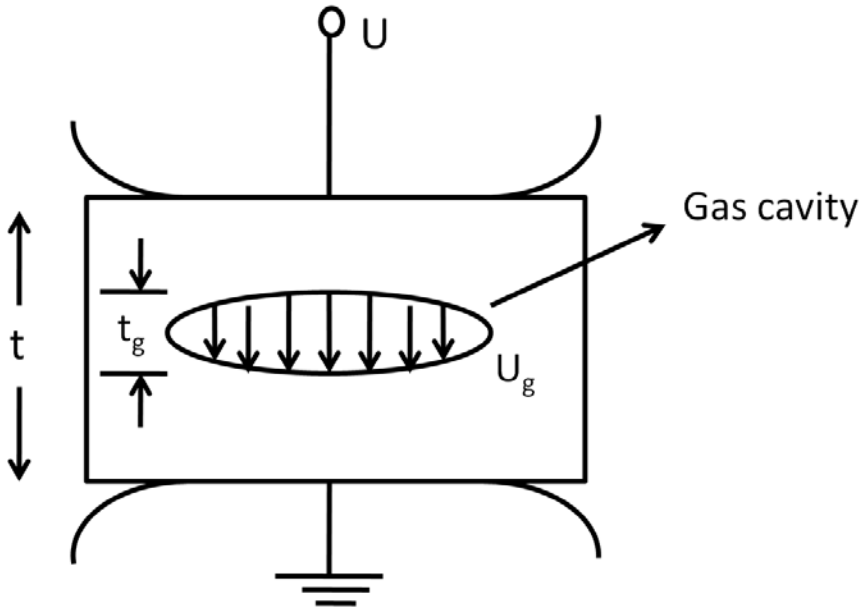

Figure 2.1(c) Gas cavity in solid insulation.

It is seen from (1) that the air medium is stressed more than the solid insulation. If the stress is sufficient enough to cause breakdown of the air, an electric spark is generated in the air medium. Since the spark or electrical discharge is confined only to the weaker component, it is called a partial discharge (PD). Similarly unintentionally introduced gaseous media either in series or in parallel with dielectrics as shown in Fig. 2.1(b) may cause internal discharges in the air space. In Fig. 2.1(c) an air filled cavity situated in the insulation is also electrically stressed in excess of the surrounding medium and a partial breakdown initiates in the cavity [4].

2.3 Partial discharge under alternating voltage conditions

Fig. 2.2(a) shows a plane parallel specimen of insulation to which a sinusoidal electric field is applied [4]. The insulation encloses a gaseous defect inside it. The electrical equivalent circuit of the specimen is shown in Fig. 2.2(b). In the Fig. 2.2, C_0 is the capacitance of the defect; C_1 and C_2 are the capacitances of the regions indicated. In Fig. 2.2(c), closing of the switch represents starting of the partial discharge process. The instantaneous charge transferred from the higher potential point (indicated X) to the lower potential point indicated (Y) results in a very fast rising transient voltage pulse. The discharge neutralizes a certain amount of charge residing

on the walls of the cavity. Due to the neutralization, the cavity acquires a potential called the extinction voltage. The PD inception voltage is then restored upon further variation of applied voltage [4].

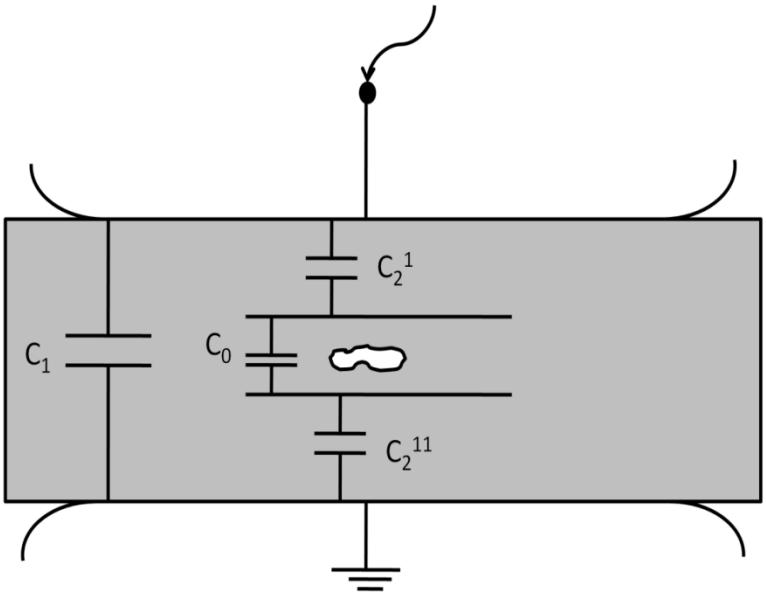

Figure 2.2(a) Gaseous defect in a solid dielectric.

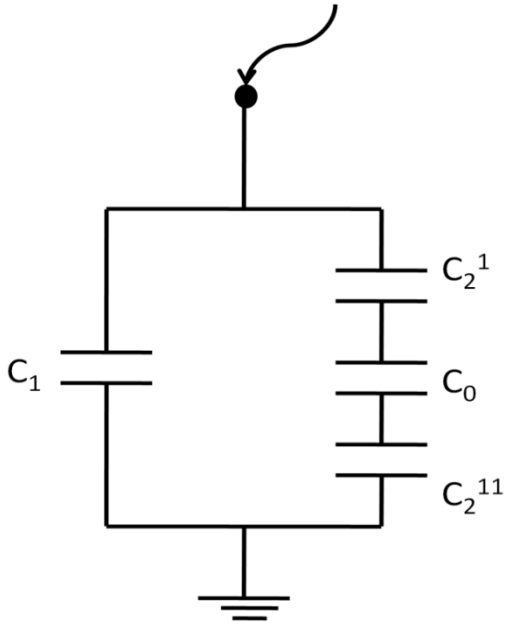

Figure 2.2(b) Equivalent circuit of Fig. 2.2(a).

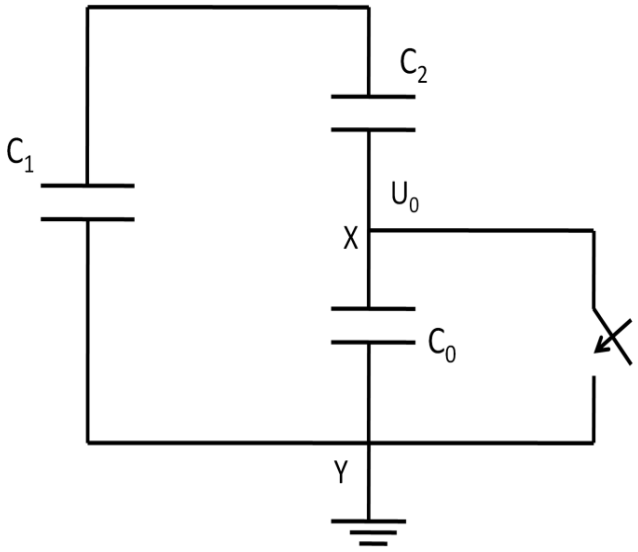

Figure 2.2(c) Equivalent circuit of partial discharge phenomenon.

2.4 Partial discharge analysis

The main difficulty involved in the PD signal analysis is to free the PD signal from surrounding noise and interferences present onsite. The two broad types of interferences that pollute the PD signals are random internal noise and externally coupled disturbances [4]. Random noise results from random fluctuations in electronic devices such as amplifiers, ICs, detection circuit impedance etc. The external interferences are further broadly classified as discrete spectral interferences (DSI), periodic pulse shaped interferences and stochastic pulse shaped interferences. The DSI results from radio transmission and power line carrier systems. The periodic pulse shaped interferences result from power electronics circuits or during periodic switching of adjustable speed thyristor drives. Stochastic pulse shaped interferences result from infrequent switching operations, arcing between metallic contacts etc. [4]. For rejecting the noise and interferences from the PD signal various de-noising methods are adopted. Among the de-noising methods wavelet transform is a powerful tool in extracting the PD signal from severe noise and interferences. Wavelet based de-noising can again be performed using various techniques and each has its own advantage. To evaluate the performance of a de-noising method the reference PD signal or the clean PD signal should also be known so that the de-noised result can be compared with the reference. In this work the de-noising methods are adopted on five signals having different characteristics. Among the five signals four are simulated and one is a practical PD signal obtained in laboratory. The four simulated PD signals are used to evaluate the

de-noising performance of a de-noising method. As there is no reference signal for the practical signal, the de-noising performance index used for it is different from the simulated signals. The simulation of the four PD signals is carried out below.

2.5 Simulation of noisy PD signals

In practical measurements, PD voltage signals are captured by passing the current through a detection circuit. So the detected voltage signals generally possess different pulse shapes depending up on the type of detection circuit. The detection circuits are realized using either RC impedance circuit or RLC impedance circuits. The output voltage pulse in RC impedance circuit is represented as a damped exponential pulse (DEP) and the output voltage pulse in RLC impedance circuit is represented as a damped oscillatory pulse (DOP) [2]. Considering the shape of a PD current pulse and the type of detection circuits, the DEP and the DOP can be numerically simulated [2] as (2) and (3) respectively.

$$DEP(t) = A(e^{-(t-t_0)/t_1} - e^{-(t-t_0)/t_2}) \tag{2}$$

$$DOP(t) = A\sin(2\pi f_c(t-t_0))(e^{-(t-t_0)/t_1} - e^{-(t-t_0)/t_2}) \tag{3}$$

where, A represents the pulse peak value, t_1, t_2 are damping coefficients, t_0 is the time of occurrence and f_c is the oscillatory frequency of the DOP. Two PD signals, one carrying 4 DEP type pulses shown in Fig. 2.3 (a) and other carrying 4 DOP type pulses shown in Fig. 2.4 (a), are simulated using (2), (3) and the values in Table 2.1. Values of A and f_c are fixed at 5 mV and 100 kHz respectively. The sampling rate is 5 MHz. To simulate noisy PD signals, the DEP and DOP type signals are noised by white Gaussian noise (WGN) at signal to noise ratio (SNR) -5dB. The noisy DEP and DOP type signals generated after the addition of WGN are shown in Fig. 2.3(b) and Fig. 2.4(b) respectively. To simulate PD signals severely corrupted by both noise and interference, the DEP and DOP type signals are corrupted by WGN at -10 dB and discrete spectral interference (DSI). Here the DSI is generated by the combination of a series of amplitude modulated signals [3] described as

$$e(t) = \sum_{i=1}^{5}(c + m\times\sin(2\pi f_m t))\times\sin(2\pi f_i t) \tag{4}$$

where, c is the amplitude of the carrier wave, m is the amplitude of modulating signal, f_m the frequency of modulating signal, f_i the frequency of the carrier wave. In the simulation the

parameters used are c =1, m=0.4, f_m =1 kHz, f_i =400 kHz, 500 kHz, 600 kHz, 700 kHz, 800 kHz, respectively. The DSIs are generated as amplitude modulated sine waves with 40% modulation and a constant modulating frequency of 1 kHz. The interference to noise ratios (INR) for the signals are given in Table 2.2. The WGN and DSI corrupted DEP and DOP type signals are shown in Fig. 2.3(c) and Fig. 2.4(c) respectively. In this thesis the DEP and DOP type signals corrupted with WGN at SNR -5 dB are called the DEP type signal-1 and DOP type signal-1 respectively. The DEP and DOP type signals corrupted with WGN at SNR -10 dB and DSI are called the DEP type signal-2 and DOP type signal-2 respectively. A practical PD signal obtained at 9 kV voltage using transformer oil as the dielectric specimen is shown in Fig. 2.5. Sampling frequency of the practical signal is 99.950 kHz (approximately 0.1 MHz).

TABLE 2.1

PARAMETERS OF SIMULATED PD SIGNALS

Signal Type	Pulse No.	$t_0(\mu s)$	$t_1(\mu s)$	$t_2(\mu s)$
DEP	1	100	2	0.1
	2	300	2	0.5
	3	700	5	0.6
	4	900	2	0.8
DOP	1	100	5	0.1
	2	400	4	0.1
	3	600	2	0.5
	4	900	5	2

TABLE 2.2

CHARACTERISTICS OF DSI USED IN SIMULATION

f (kHz)	400	500	600	700	800
INR(dB) (DEP)	-1.78	4.24	-7.8	1.74	6.18
INR (dB) (DOP)	7.29	8.58	0.91	-14.6	-2.6

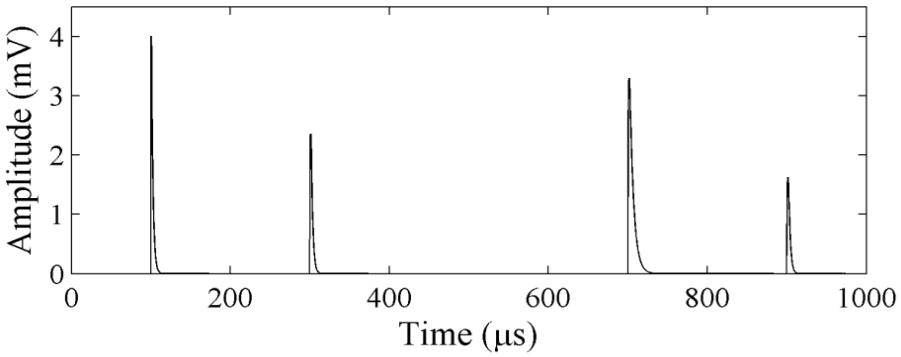

Figure 2.3(a) Damped exponential pulse (DEP) type signal.

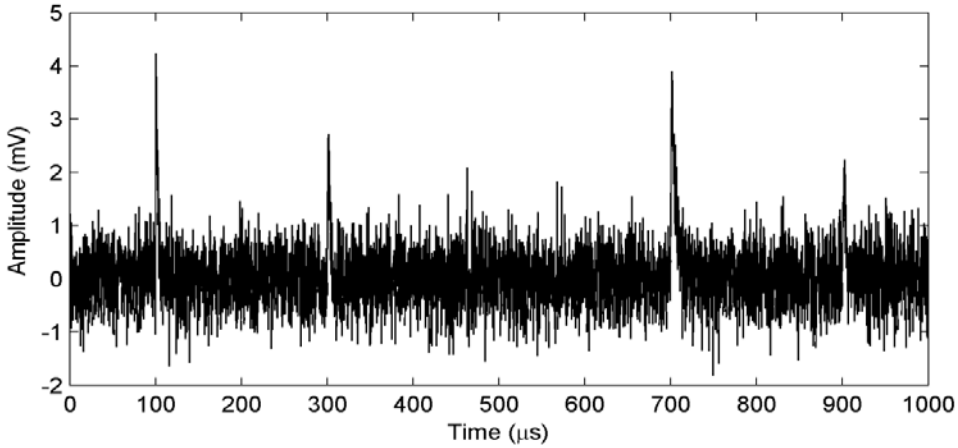

Figure 2.3(b) DEP type signal corrupted by white Gaussian noise (WGN) at SNR -5 dB.

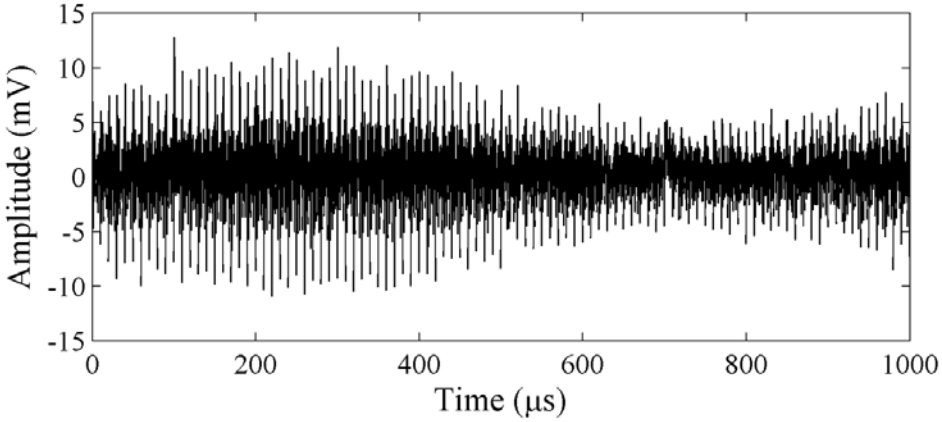

Figure 2.3(c) DEP type signal corrupted by WGN at SNR -10 dB and Discrete spectral interferences.

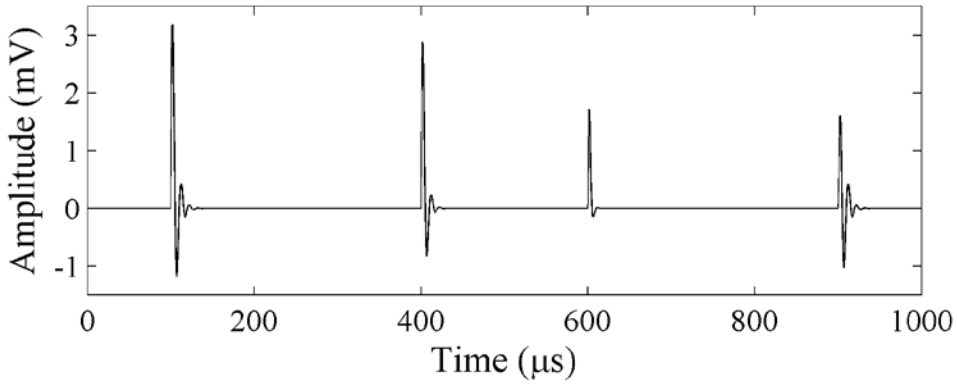

Figure 2.4(a) Damped oscillatory pulse (DOP) type signal.

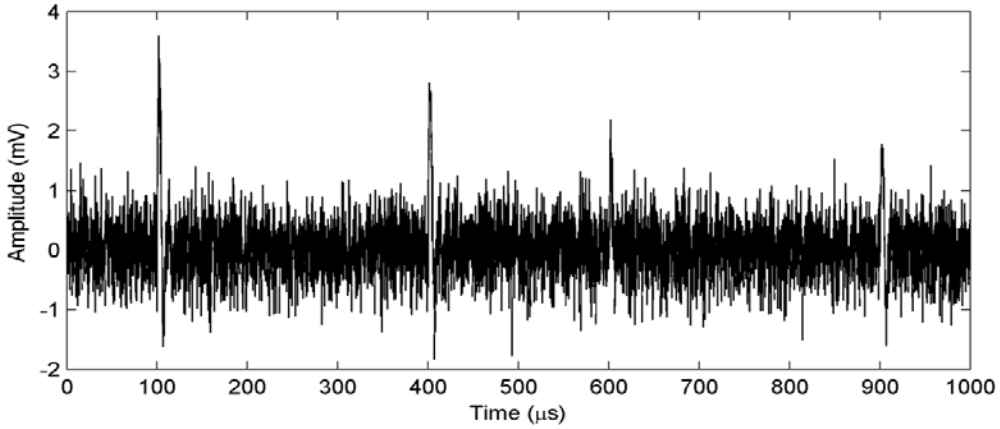

Figure 2.4(b) DOP type signal corrupted by white Gaussian noise (WGN) at SNR -5 dB.

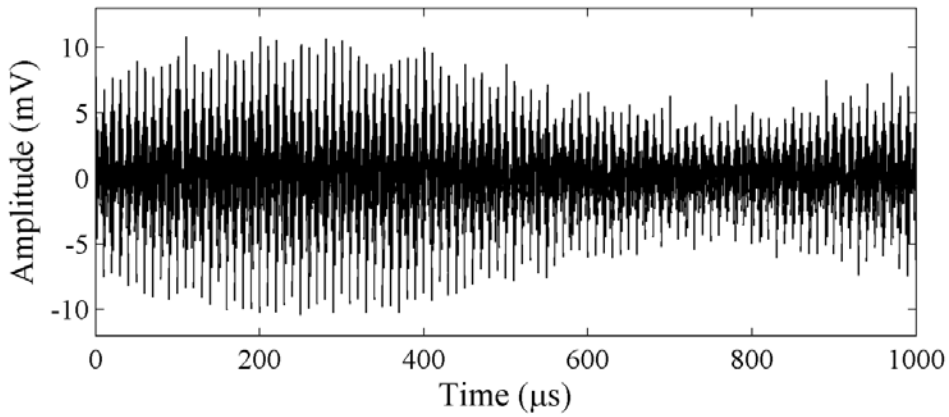

Figure 2.4(c) DOP type signal corrupted by WGN at SNR -10 dB and Discrete spectral interferences.

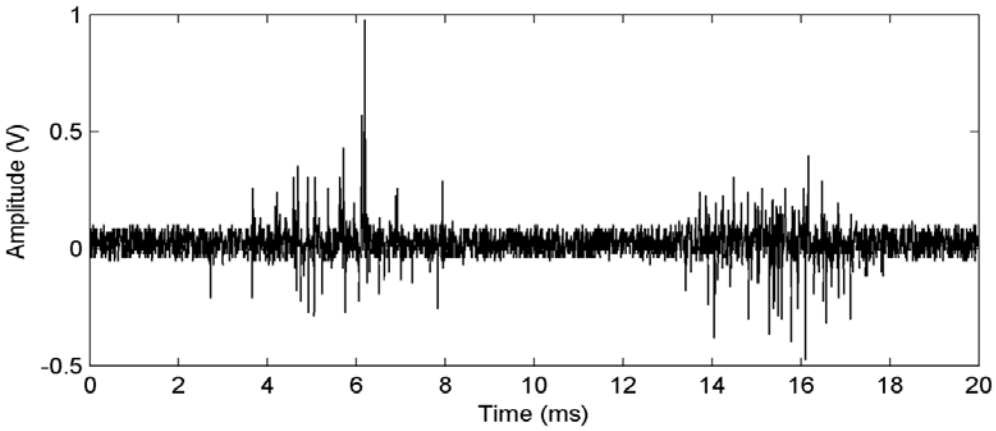

Figure 2.5. A practical PD signal obtained in high voltage laboratory using transformer oil as the dielectric specimen and applied voltage of 9 kV.

2.6 Summary

Using PD signal analysis, condition of Insulation in HV power equipments can be studied. During onsite and online PD measurements, noise and interference corrupt the acquired PD signal. Among the different de-noising techniques adopted to extract the PD signal, wavelet based techniques are superior. However, to determine the effectiveness of the wavelet based techniques it is required to evaluate the method by applying it on simulated noisy PD signals. The noisy PD signals are simulated numerically.

Chapter 3
De-noising of PD Signals using Discrete Wavelet Transform

3.1 Introduction

Nowadays with the advent of digital techniques, PD measurements are performed onsite and online [1]. The drawback of such measurement is that the acquired PD signal is corrupted by the surrounding noise and interferences. Hence the PD pulses to be analyzed get buried in the severe noise. The large amplitude of amplitude modulation interference buries the signal inside it. Hence various time domain and frequency domain de-noising techniques are adopted to extract the PD pulses from such noise and interferences. Recently wavelet transform (WT) has emerged as a powerful tool for the extraction of PD signals. Wavelet transform uses wavelet function as the basis function which scales itself according to the frequency under analysis. The scheme shows better results because the basis function used in WT is a wavelet instead of an exponential function used in FT and STFT. The aim of PD signal de-noising is to retain the PD pulses and rejecting the noise and interferences. Using WT the signal is decomposed into different frequency levels and presented as wavelet coefficients. The more similarity occurs between the wavelet and the PD structure, more is the coefficient's absolute value. So those coefficients which are of less magnitudes are thresholded to zero and the rest are retained. The modified coefficients are then used to rebuild the signal, which represents the de-noised PD signal. Depending on the types of signal, continuous wavelet transform (CWT) and discrete wavelet transform (DWT) are employed. For continuous time signal, CWT based de-noising is adopted and for discrete time signal DWT based de-noising is adopted. In this work all the signals shown are discrete in nature. Hence DWT is employed to de-noise the simulated and practical PD signals [6].

3.2 Continuous wavelet transform (CWT)

Continuous wavelet transform (CWT) is employed for continuous time signals. It uses a wavelet as its basis function. The wavelet chosen is called the mother wavelet. The scaled and translated versions of the mother wavelet are multiplied with the signal to be de-noised, to

generate wavelet coefficients at different decomposition levels. The *CWT* of a signal *x(t)* is mathematically given as [5]:

$$CWT(a,b) = \frac{1}{\sqrt{a}} \int_{-\infty}^{\infty} x(t) g\left(\frac{t-b}{a}\right) dt \tag{5}$$

where, a is the scale factor and *b* is the translation factor. Both *a* and *b* are continuous in nature. *g(t)* is the mother wavelet chosen. The scaling factor *a* is inversely related to frequency. It means that if the frequency under analysis is high, then it compresses itself and if the frequency under analysis is small then it expands. As can be seen the WT maps the signal *x(t)* to a two dimensional space. With the number of de-composition level, the scaling factor *a* changes to de-compose the signal to corresponding frequency level. At a particular scale *a*, the signal translates over continuous time to give wavelet coefficients. Effectiveness of the WT generally depends on the mother wavelet chosen from the wavelet library. There are many wavelets available like Haar, Daubechies, Morlet, Symlet etc. One of the most widely used mother wavelets is Daubechies wavelet which suits the requirements for the application in power system [5].

3.3 Discrete wavelet transform (DWT)

Wavelet analysis of a discrete time signal is carried out by DWT. Discrete wavelet transform is derived from CWT by substituting $a = a_0^{\,m}$ and $b = nb_0a_0^{\,m}$. DWT of a discrete time signal x[n] is defined as [5]

$$DWT(m,k) = \frac{1}{\sqrt{a_0^{\,m}}} \sum_n x[n] g\left[\frac{k - nb_0a_0^{\,m}}{a_0^{\,m}}\right] \tag{6}$$

where, *g* is the mother wavelet. *k* is an integer used to refer a sample. Hence in DWT, *a* and *b* vary in a discrete manner. Unlike CWT, the scaling used in DWT gives logarithmic frequency coverage [5]. Interchanging the *n, k* in (6) and after the rearrangement of the DWT, (7) gives:

$$DWT(m,n) = \frac{1}{\sqrt{a_0^{\,m}}} \sum_k x[k] g[a_0^{\,-m} n - b_0 k] \tag{7}$$

It can be seen that (7) resembles the convolution of a signal with the impulse response h[n] of an FIR filter. The convolution formula is given as

$$y(n) = \frac{1}{c}\sum x[k]h[n-k] \tag{8}$$

From equation (7) and (8) it can be seen that the impulse response of the DWT filter is $g[a_0^{-m}n - b_0k]$. For a_0=2 or (a_0^{-m} = 1, 1/2, 1/4, 1/8.....), and b_0 = 1, the DWT can be implemented using a low pass filter l[n] and high pass filter h[n] as shown in Fig. 3.1. In the Fig. 3.1(a) a signal x[n] is fed to the low pass and high pass filters. Then the outputs of the two filters are downsampled by a factor 2 to obtain the DWT coefficients. The result obtained after downsampling the output of high pass filter are called detail coefficients and that of low pass are called approximation coefficients. The approximation is further fed to the low pass and high pass filter and the process is iterated. The high pass and low pass filters are related by (9):

$$h[L-1-n] = (-1)^n l[n] \tag{9}$$

where, L is the length of the filter. The filters are known as quadrature mirror filters (QMF) [5].

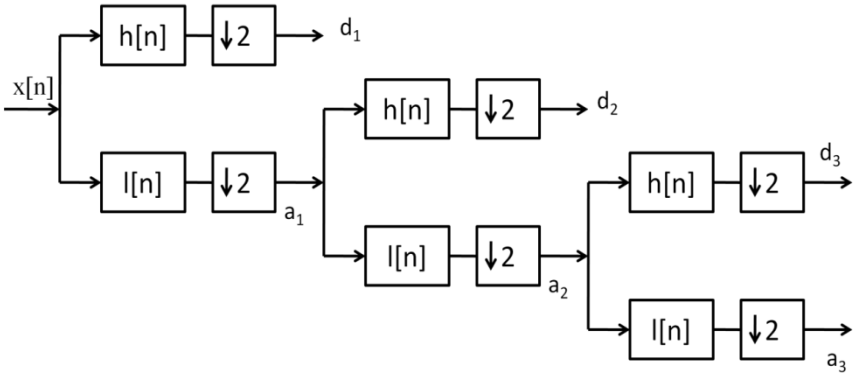

Figure 3.1(a) Block diagram of DWT decomposition.

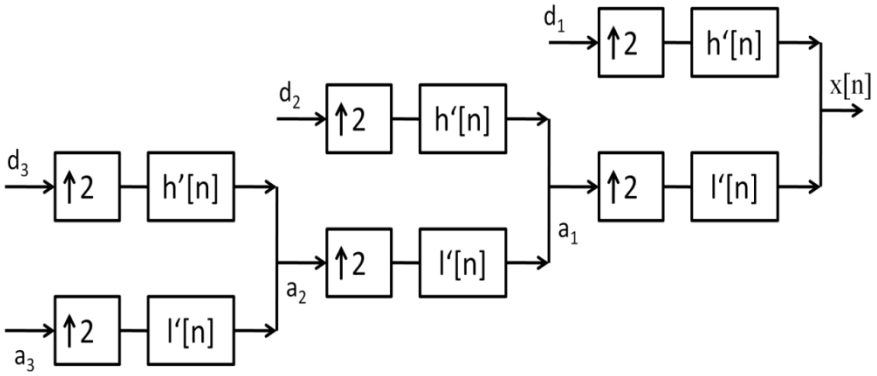

Figure 3.1(b) Block diagram of DWT reconstruction.

3.4 De-noising of PD signals using DWT

The traditional DWT based de-noising method involves determination of the DWT coefficients for a given signal, then adopting thresholding of the DWT coefficients followed by reconstruction of the signal by taking the inverse wavelet transform of the modified DWT coefficients. This thresholding function adopted can be soft or hard thresholding. The Multi-resolution Signal Decomposition (MSD) feature associated with the DWT makes it possible to retain the coefficients representing the signal and rejecting the others. During the DWT based de-noising of a PD signal choice of some parameters has to be made. The choice of mother wavelet, selection of maximum decomposition level and, thresholding rule and thresholding function selection are some of the vital issues in the implementation of DWT. Careful selection of the mentioned parameters gives more accurate de-noising results [1]. They are briefly discussed below:

3.4.1 Selection of mother wavelet

Accuracy of DWT based de-noising results depends on the selection of the mother wavelet. Generally a wavelet gives better de-noising results if its shape is similar to the shape of the PD pulse to be extracted. Selection of mother wavelet can be scale independent and scale dependent. In the scale independent mother wavelet selection, a single wavelet is employed for all the decomposition levels, where as in level dependent wavelet selection, for each level, the suitability of a wavelet as the mother wavelet is tested. In [2] it is mentioned that db2 (Daubechies wavelet of order 2) and db7 (Daubechies wavelet of order 7) are the most suitable wavelets for the wavelet analysis of DEP and DOP type signals respectively.

3.4.1.1 Energy distribution based mother wavelet selection

This method is a scale independent mother wavelet selection method. Generally scale independent mother wavelet is chosen based on trial-and-error and guided by hints published in literatures on PD signal de-noising [1]. In [1-3] Daubechies wavelets have been found most suitable for the PD signal analysis. In [3] an energy distribution based scale independent mother wavelet selection method is proposed. In fact, the splitting of frequency bands by DWT filter pair is not ideal. So overlapping between low pass and high pass filter exists in the DWT. The QMF frequency response varies with mother wavelets resulting in signal energy distribution depending on the chosen mother wavelet [3]. Hence the signal is decomposed up to a certain

level using various wavelets and the energy at each level is calculated. The wavelet that concentrates the energy at a particular level more than the others is chosen as the mother wavelet.

3.4.1.2 Scale dependent mother wavelet selection

For the scale-dependent mother wavelet selection an energy based wavelet selection (EBWS) method is proposed in [7]. According to the method a wavelet is selected as an optimal wavelet at level *j*, if decomposition by using the wavelet generates a_j of *x* with greater energy percentage than by using any other wavelets. The method is based on the fact that when the detail coefficients of a level are made zero, the signal also loses its energy corresponding to that level and hence de-noised waveform distortion occurs. So if a wavelet can generate approximation of the PD signal with more energy percentage than all other wavelets, the wavelet is chosen as the mother wavelet. As the detail's energy percentage is smaller now, the de-noised PD signal loses less energy and the waveform distortion is less. The optimal wavelet selection is made for each scale and is thus scale dependent. Given a wavelet library $\{g_i : i=1, 2, \cdots, N\}$ and the highest decomposition level *J*, the scale dependent wavelet selection is as follows [7]:

1) A wavelet g_i is selected from the wavelet library. A one-level decomposition of *x* is performed. This is considered as the first level wavelet decomposition. The approximation and detail $a_1^{\,i}$ and $d_1^{\,i}$ are obtained.

2) $E_{a1}^{\,i}$, the energy percentage of $a_1^{\,i}$ defined in (10) is calculated until *i*=*N*.

$$E_a = \frac{\sum_k a_{J,k}^{\,2}}{\sum_k a_{J,k}^{\,2} + \sum_j \sum_k d_{j,k}^{\,2}} \tag{10}$$

3) If $E_{a1}^{\,p}$ is the maximum of $E_{a1}^{\,i}$, where *i*=1, 2, ⋯, *N*, the wavelet g_p is the optimal wavelet for the first decomposition level.

4) For the *j*th level decomposition, let $x = a_{j-1}^{\,p}$, where $a_{j-1}^{\,p}$ is the approximation decomposed by the optimal base wavelet g_p at level *j*-1. A wavelet g_i is selected and one-level wavelet decomposition of the updated *x* is carried out to obtain $a_j^{\,i}$.

5) Then $E_{aj}^{\,i}$, the energy percentage of $a_j^{\,i}$ is calculated until *i*=*N*.

6) The maximum of $E_{aj}^{\ i}$, where *i*=1, 2, ⋯, *N* is calculated. The wavelet g_i corresponding to the maximum is selected as the optimal mother wavelet for the *j*th level decomposition.

7) Steps 3 to 6 are repeated until *j*=*J* and the optimal mother wavelets for decomposition at all scales are obtained.

3.4.2 Selection of maximum decomposition level

In the DWT, the maximum decomposition level of a signal is determined by $J_{ful} = fix(\log_2 n)$, where *n* is the length of the signal, *fix* rounds the value in the bracket to its nearest integer. However in this work as MATLAB wavelet toolbox is employed, the signal length at the highest level of decomposition should not be less than the length of the wavelet filter being used. So the maximum decomposition level $J_{\max}$ for a signal is given as

$$J_{\max} = fix\left(\log_2\left(\frac{n}{n_w}-1\right)\right) \tag{11}$$

where, *n* is the length of the signal, n_w is the length of the decomposition filter associated with the chosen mother wavelet [3]. However in practice maximum decomposition level for a wavelet based de-noising is selected according to the convenience and requirement.

3.4.3 Selection of thresholding rule

Selection of threshold value is crucial in wavelet based PD signal de-noising. Careful rejection of the coefficients representing noise improves the accuracy of the de-noising results. The various thresholding rules adopted for wavelet based de-noising are mentioned below:

3.4.3.1 Automatic thresholding rule

The challenge involved in thresholding during wavelet-based PD signal de-noising is to automate the process of "thresholding" so that less involvement of human judgment is required. In [6] an automatic thresholding rule is proposed as:

$$\lambda_j = \frac{m_j}{0.6745}(\sqrt{2\times\log_e(n_j)} \tag{12}$$

where, λ_j is the threshold value at level *j*, m_j, the median value of the coefficients at level *j*, and n_j is the number of coefficients associated with level *j*.

3.4.3.2 Reconstruction based thresholding

In [1] a reconstructed time-domain components based de-noising method is proposed. The method decomposes the signal in to detail and approximation coefficients at various levels. Then all the details and the last level approximation coefficients are reconstructed to obtain time-domain reconstructed detail and approximation components. Now using visual inspection the location of the PD pulses at various components is determined. And the components representing PD signal are added to obtain the de-noised signal.

3.4.3.3 Visual inspection based thresholding

This method also uses the time-domain reconstructed detail and approximation components [1] for the process of thresholding. However instead of directly adding the reconstructed components that represent the signal, the corresponding detail and approximation coefficients are thresholded suitably to extract the PD pulses with less noise. For the cases where reconstructed components are not available, threshold values are determined by visual inspection of the coefficients.

3.4.4 Selection of thresholding function

Thresholding on the DWT coefficients during wavelet based de-noising methods can be performed using either hard or soft thresholding. Hard thresholding is defined below:

$$\delta_{\lambda}^{H}(x) = \begin{cases} x & if\ |x| > \lambda \\ 0 & if\ |x| \le \lambda \end{cases} \tag{13}$$

Soft thresholding is defined as:

$$\delta_{\lambda}^{S}(x) = \begin{cases} x - \lambda & if\ x > \lambda \\ 0 & if\ |x| \le \lambda \\ x + \lambda & if\ x < -\lambda \end{cases} \tag{14}$$

where, λ is the threshold value and δ_{λ}^{H} , δ_{λ}^{S} are the thresholded coefficients. Hard thresholding is preferred in PD de-noising, as the higher coefficients values associated with the PD signal are kept without any modification which results in an improved PD signal to noise ratio [8].

3.5 De-noising performance indices

The PD de-noising methods aim to reject the noise and interferences and retain the PD pulses. However the accuracy in de-noising results depends on the severity of noise, mother

wavelet chosen, maximum decomposition level taken, thresholding rule adopted and the thresholding function employed etc. Also if there is a noisy component having features similar to the PD pulse then the PD pulse is also affected during thresholding. Hence the recovered PD signal deviates from the signal to be extracted. The extracted pulses get attenuated and distorted during the de-noising process. It is always desirable to extract the PD pulses with less distortion and attenuation. To quantify the de-noising results and to measure the effectiveness of the de-noising methods various de-noising performance indices are described below:

3.5.1 Change in PD pulse amplitude:

The percentage change in PD pulse amplitude of the de-noised signal with respect to the reference signal is given by amplitude error $(\%AE)$

$$\%AE = \frac{X - Y}{X} \times 100 \tag{15}$$

where, X is the peak amplitude (positive going peak in this case) of the reference PD pulse and Y is the peak amplitude of the de-noised PD pulse [1].

3.5.2 Mean square error:

Effectiveness of a de-noising scheme is also evaluated by mean square error (MSE) defined as

$$MSE = \frac{1}{N}\sum_{i=1}^{N}(F(i) - R(i))^2 \tag{16}$$

where, N is the length of the PD signal, F represents the reference PD signal and R, the de-noised PD signal [3].

3.5.3 Signal to noise ratio:

The signal to noise ratio (SNR) is defined as

$$SNR(dB) = 10\log_{10}\frac{\sum_{i=1}^{N}F^2(i)}{\sum_{i=1}^{N}(F(i) - R(i))^2} \tag{17}$$

where, F is the reference PD signal, R is de-noised PD signal and N is the length of the PD signal.

3.5.4 Reduction in noise level (RNL)

In case of practical signal there is no reference signal, so the above three performance indices are not applicable to practical signal and only the extent of noise suppressed can be calculated. The normalized noise reduction [1] is calculated as

$$RNL\,(dB) = 10 \times \log_{10} \sum_{i=1}^{N} \frac{1}{N} (Z(i) - Y(i))^2 \tag{18}$$

where, *Z(i)* is the noisy signal acquired, *Y(i)* is the de-noised signal and *N* is the length of the signal.

3.6 DWT based de-noising results of PD signals

3.6.1 Level independent mother wavelet selection

Level independent mother wavelet selection adopts a single wavelet for the decomposition of approximations at all the levels. In this work db2 mother wavelet is used to de-noise the DEP signals and db7 is used for the DOP signals for the reason mentioned in [2]. For the practical signal db7 is used. The de-noising results for the level independent mother wavelet selection methods are shown in Figs. 3.2-3.16.

3.6.1.1 Automatic thresholding rule

In this wavelet based de-noising method choice of mother wavelet is independent of the scales; it means that one mother wavelet is applied to all the decomposition levels. For the reasons mentioned in [2] DEP type signals are analyzed using db2 as the mother wavelet and DOP type signals are analyzed using db7 as the mother wavelet. Hence for better de-noising results, these two wavelets are used here for the corresponding signals. For the de-noising of the practical signal db7 is employed in this work. The de-noising results shown in Figs. 3.2-3.6 adopt automatic thresholding rule mentioned in (12). All the de-noising methods adopt decomposition of the signal up to level 7. From the results it is seen that using automatic thresholding rule the DEP type signal-1 and DOP type signal-1 are de-noised but the severely noised DEP type signal-2 and DOP type signal-2 could not be de-noised. The practical signal is also recovered using this method.

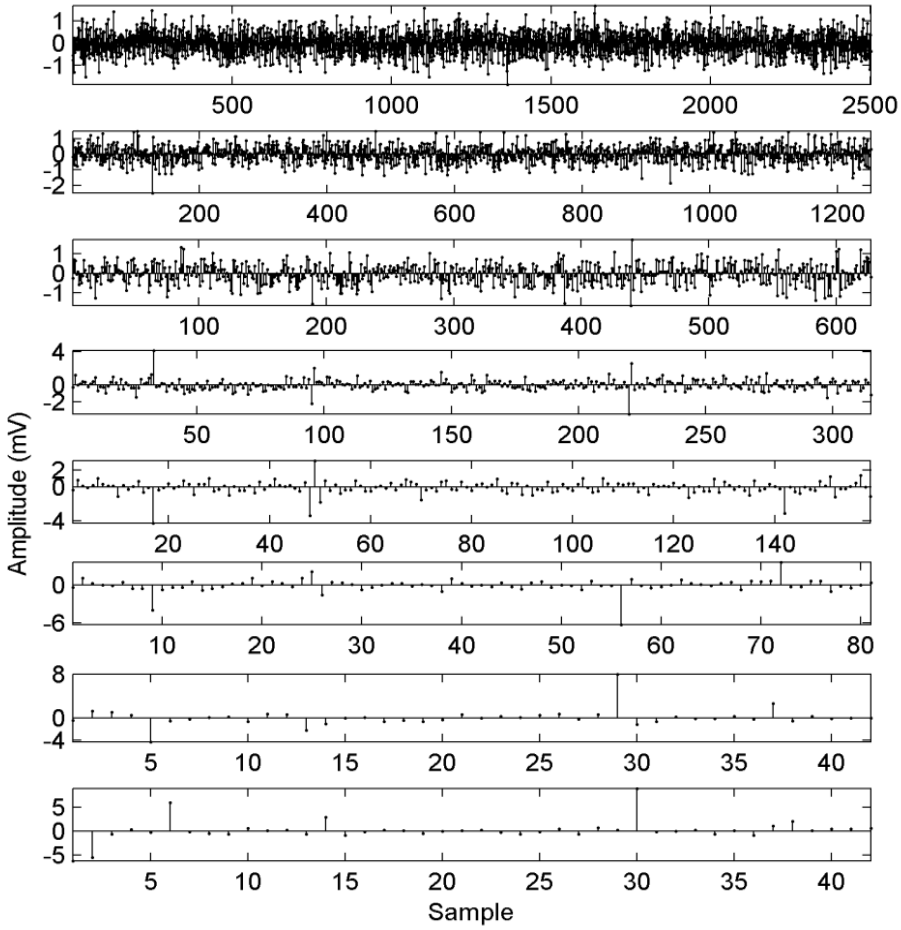

Figure 3.2(a) DWT coefficients (d1-d7, a7) of DEP type signal-1 decomposed up to level 7 using db2 mother wavelet.

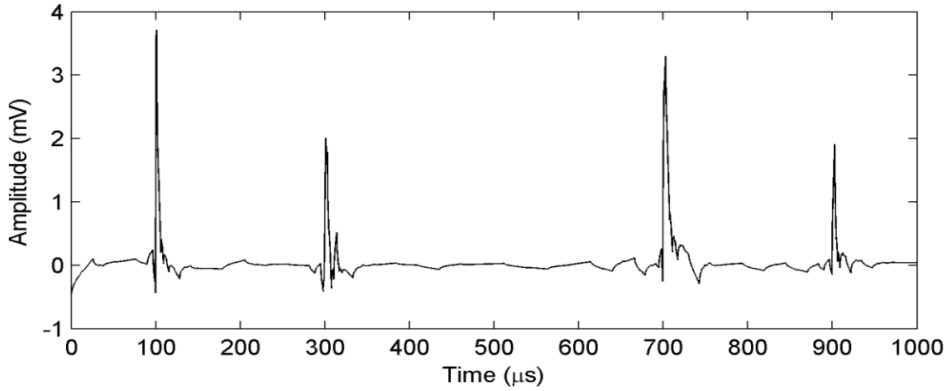

Figure 3.2(b) De-noised DEP type signal adopting automatic thresholding rule on the coefficients shown in Fig. 3.2(a).

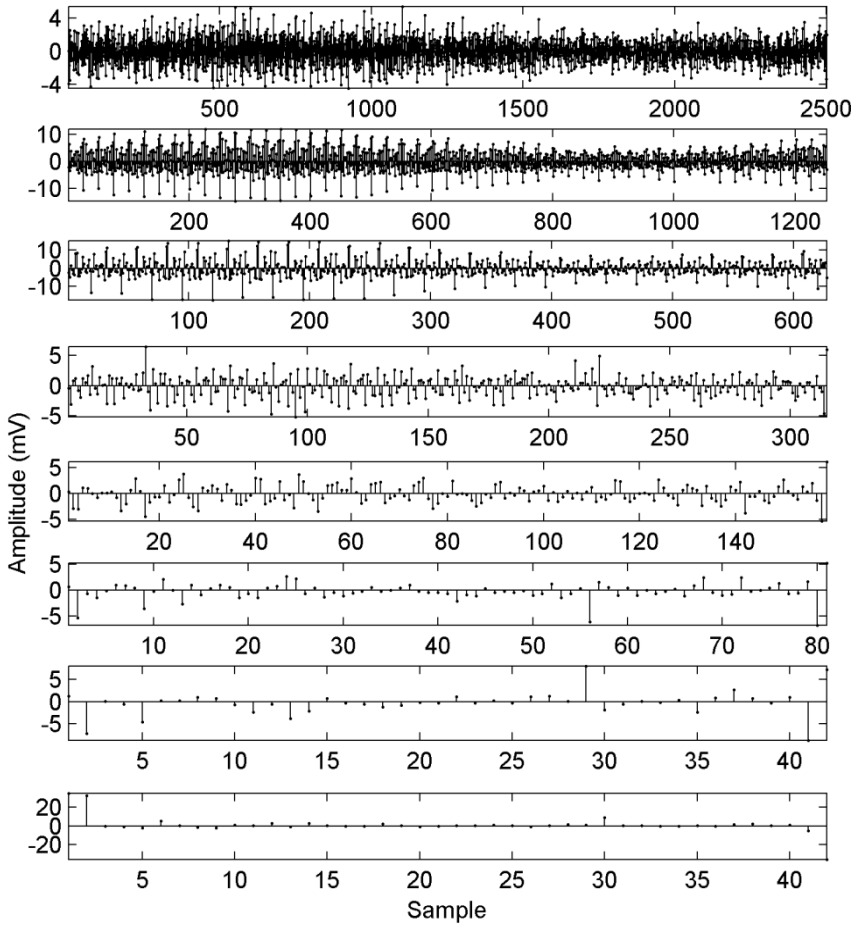

Figure 3.3(a) DWT coefficients (d1-d7, a7) of DEP type signal-2 decomposed up to level 7 using db2 mother wavelet.

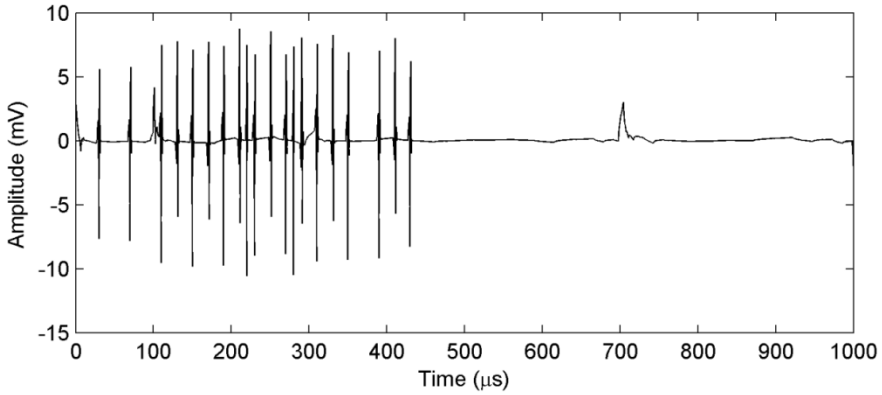

Figure 3.3(b) De-noised DEP type signal adopting automatic thresholding rule on the coefficients shown in Fig. 3.3(a).

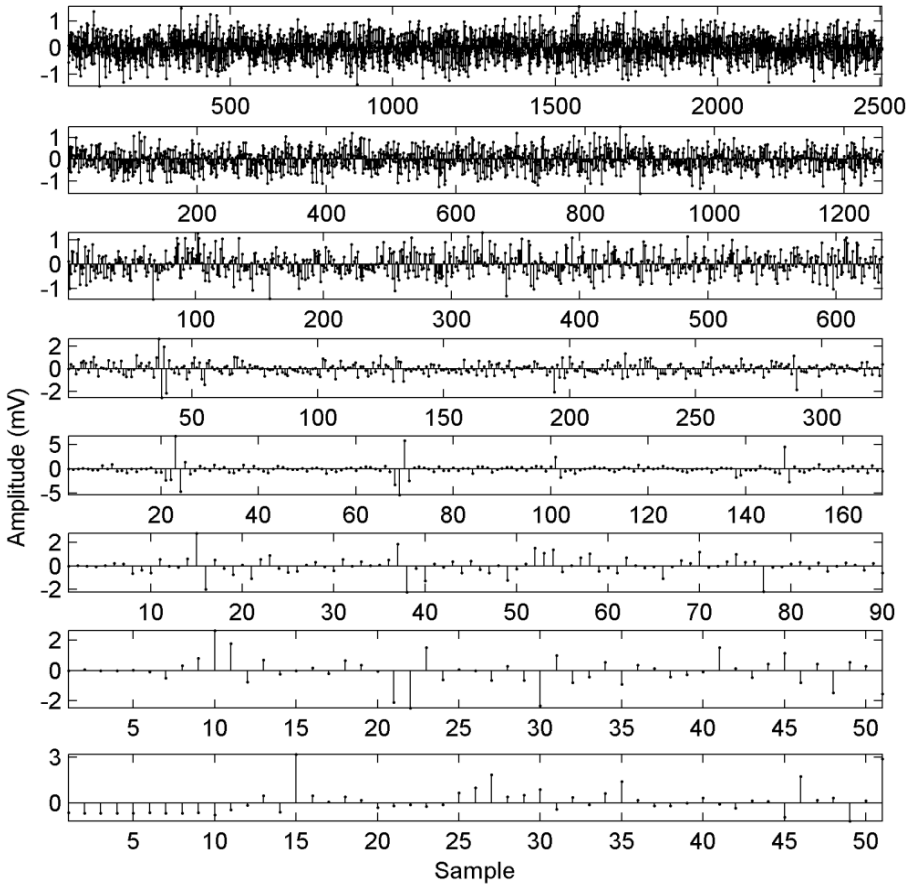

Figure 3.4(a) DWT coefficients (d1-d7, a7) of DOP type signal-1 decomposed up to level 7 using db7 mother wavelet.

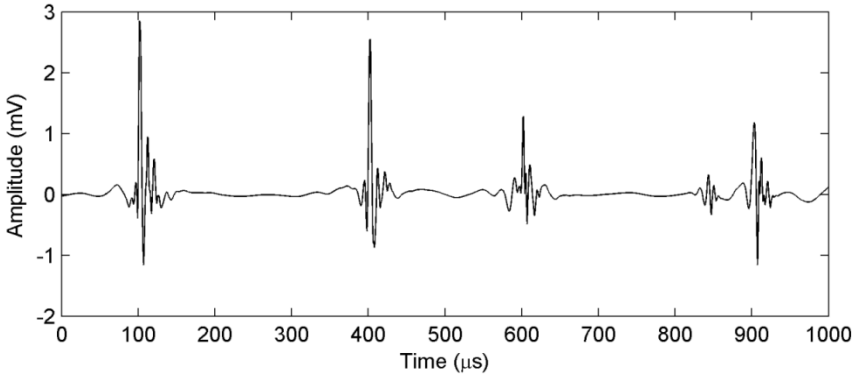

Figure 3.4(b) De-noised DOP type signal adopting automatic thresholding rule on the coefficients shown in Fig. 3.4(a).

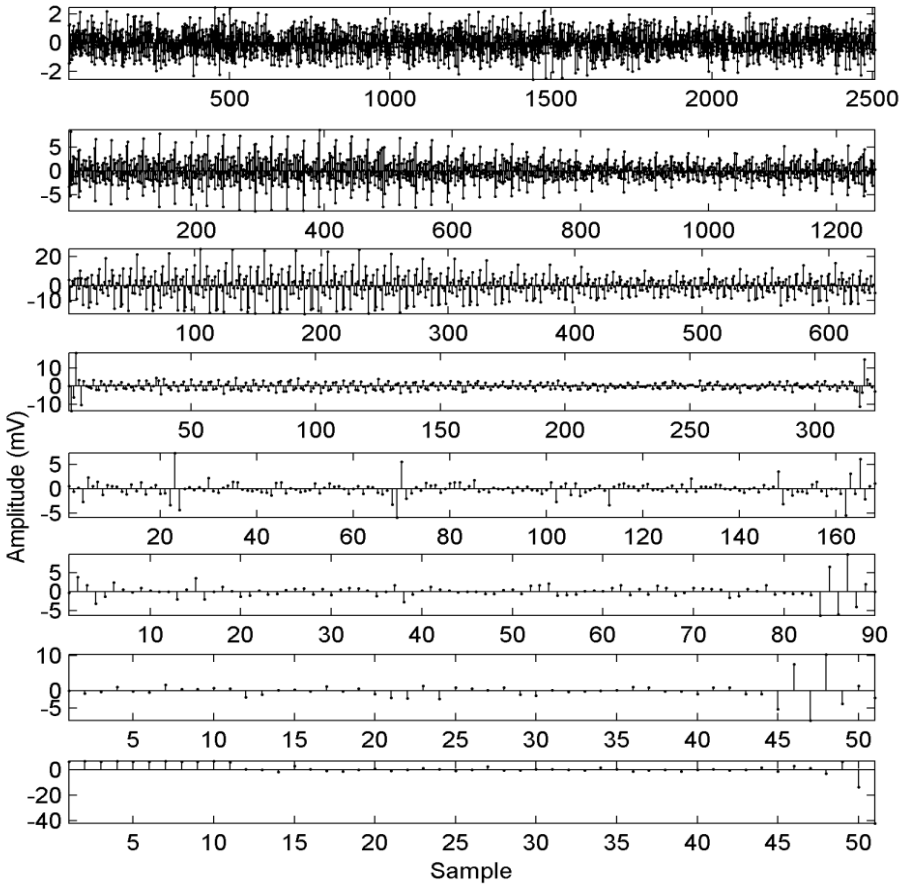

Figure 3.5(a) DWT coefficients (d1-d7, a7) of DOP type signal-2 decomposed up to level 7 using db7 mother wavelet.

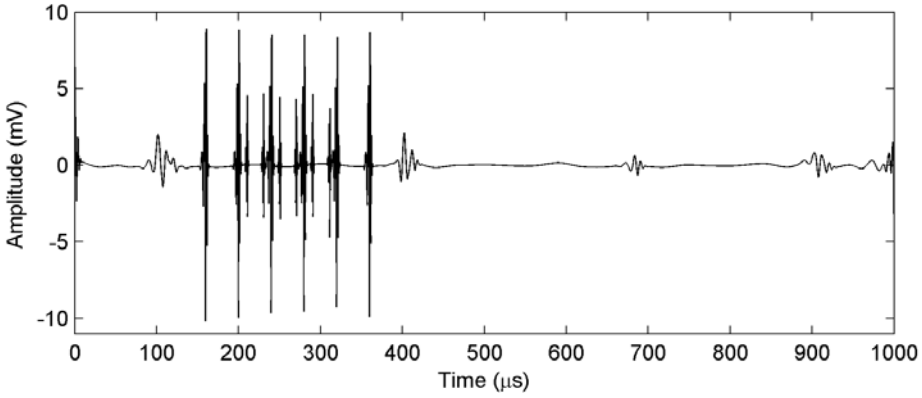

Figure 3.5(b) De-noised DOP type signal adopting automatic thresholding rule on the coefficients shown in Fig. 3.5(a).

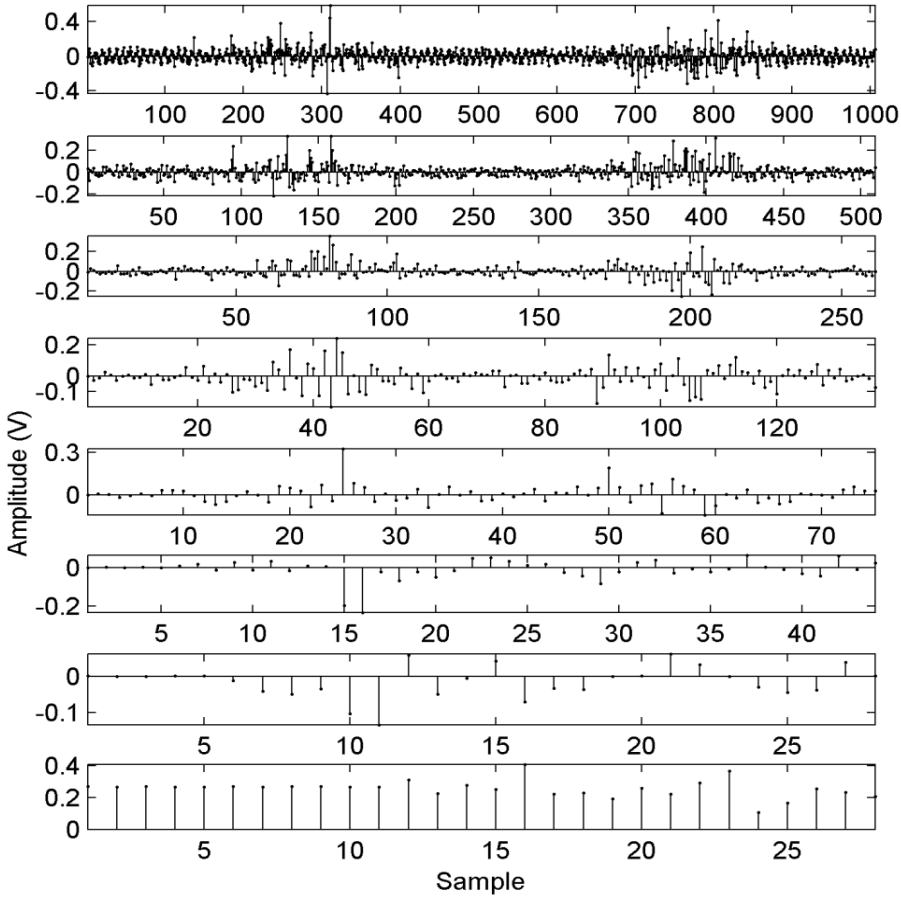

Figure 3.6(a) DWT coefficients (d1-d7, a7) of the practical signal decomposed up to level 7 using db7 mother wavelet.

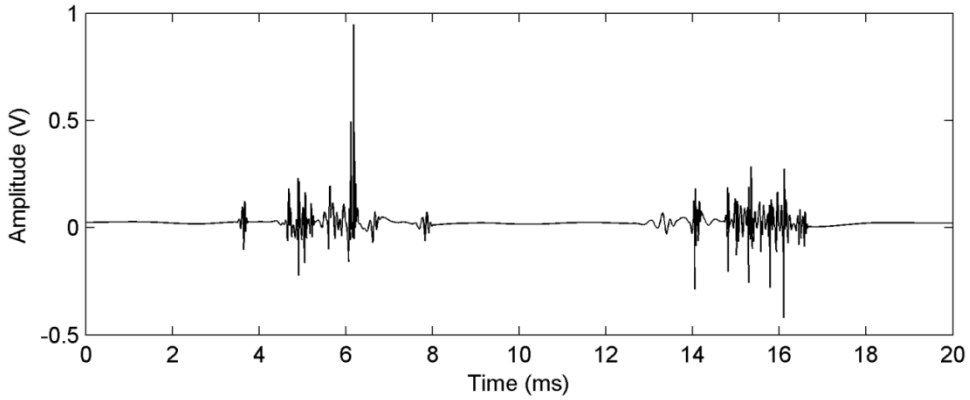

Figure 3.6(b) De-noised practical signal adopting automatic thresholding rule on the coefficients shown in Fig. 3.6(a).

3.6.1.2 Time domain reconstruction based de-noising

In this method the time domain components of the DWT detail and approximation coefficients are reconstructed. After visual inspection, the components representing the signal are added and the other components are discarded. The de-noising results of the five signals using this method are shown in Figs. 3.7-3.11. From the results it is concluded that this method works for excessively noisy PD signals. It is seen that the four pulses of DEP type signal-2 and DOP type signal-2 are identified using this method but not using the automatic thresholding rule.

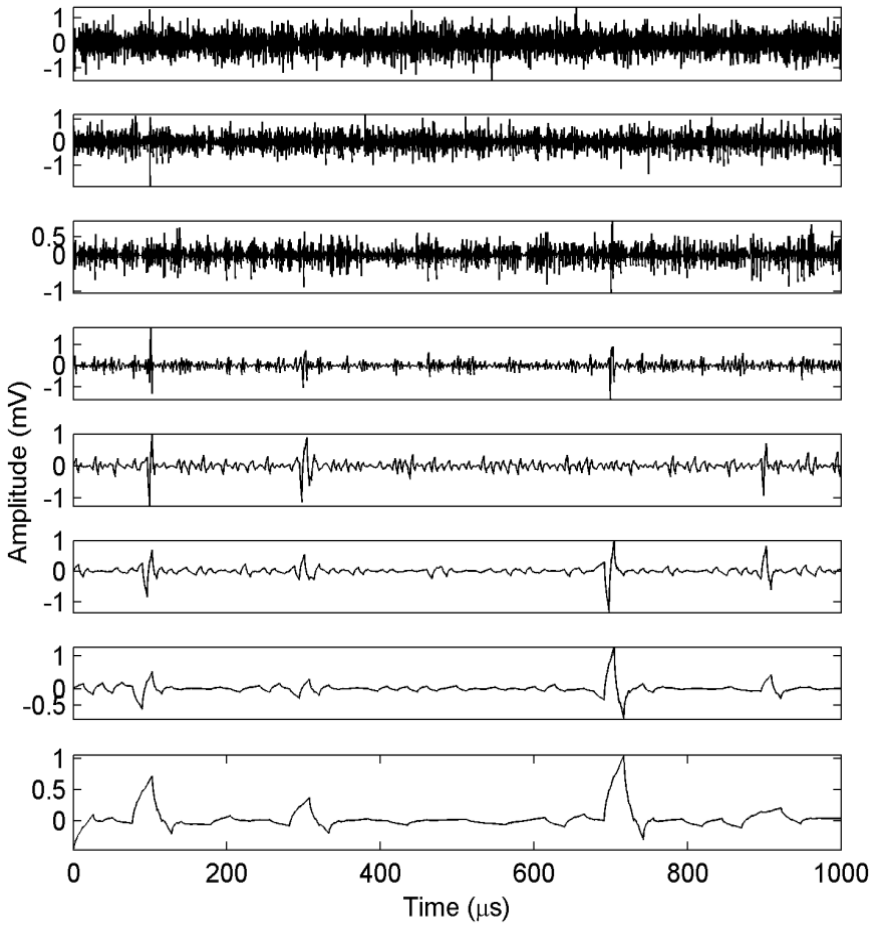

Figure 3.7(a) Reconstructed time domain components (rd1-rd7, ra7) of DEP type signal-1 DWT decomposed up to level 7 using db2 mother wavelet.

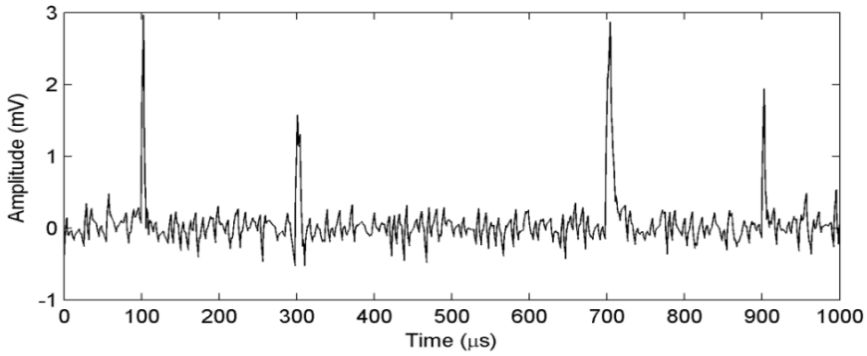

Figure 3.7(b) De-noised DEP type signal adopting reconstruction based thresholding on the time-domain components shown in Fig. 3.7(a).

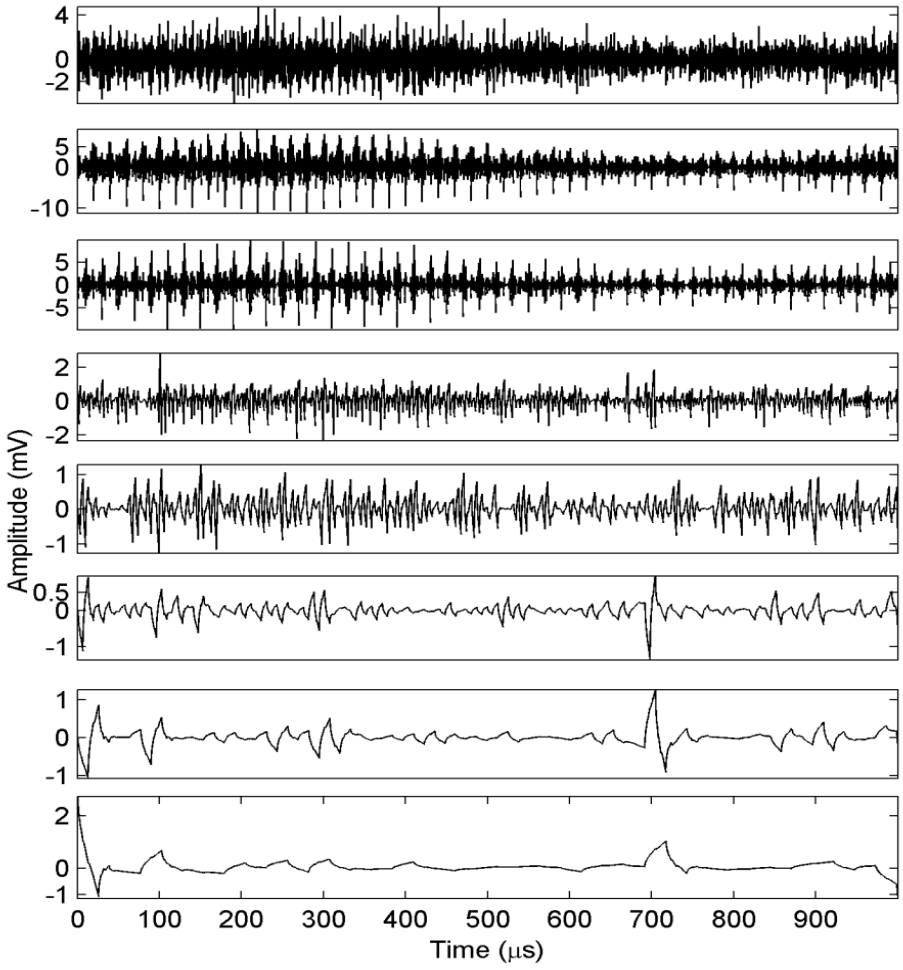

Figure 3.8(a) Reconstructed time domain components (rd1-rd7, ra7) of DEP type signal-2 DWT decomposed up to level 7 using db2 mother wavelet.

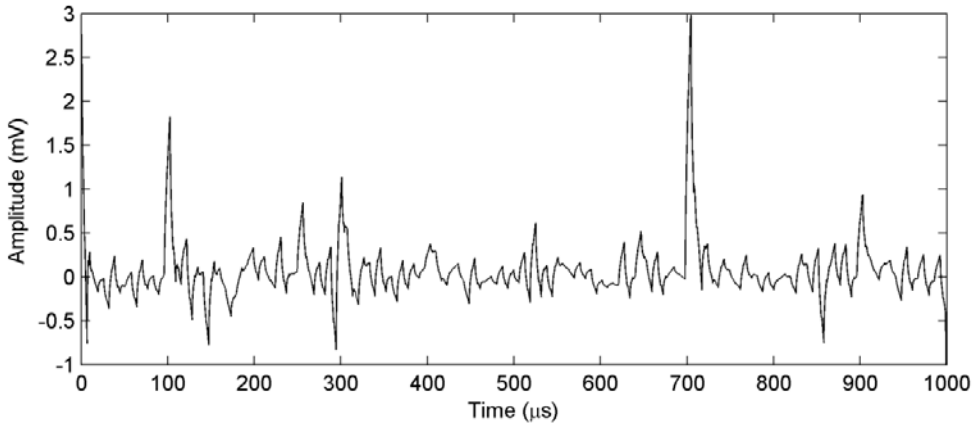

Figure 3.8(b) De-noised DEP type signal adopting reconstruction based thresholding on the time-domain components shown in Fig. 3.8(a).

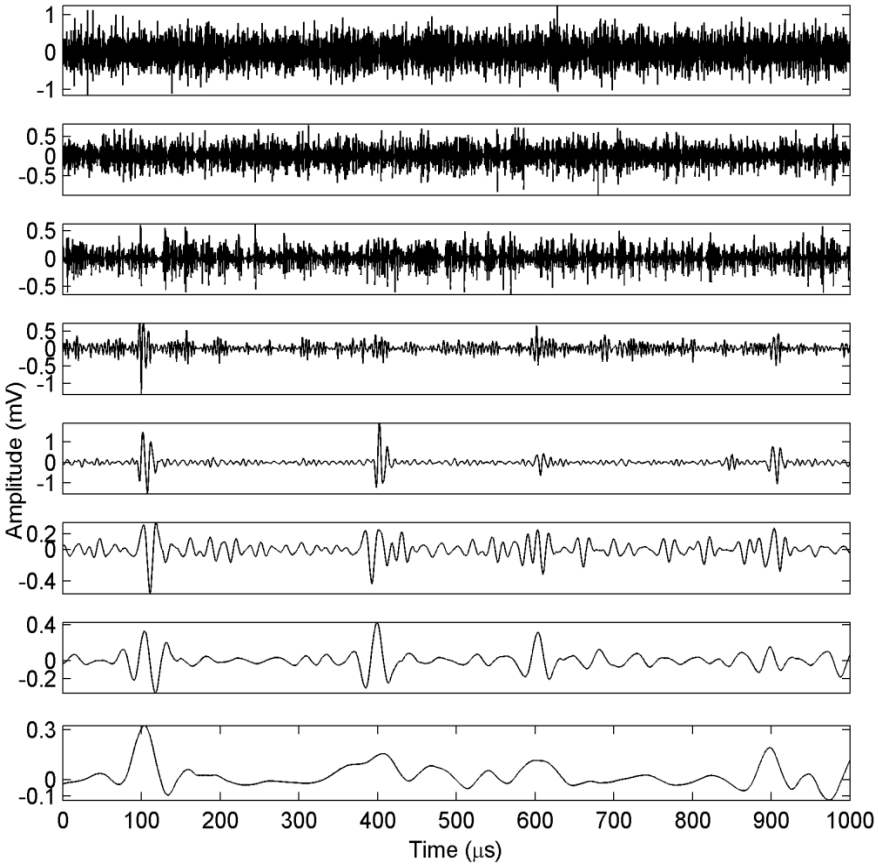

Figure 3.9(a) Reconstructed time domain components (rd1-rd7, ra7) of DOP type signal-1 DWT decomposed up to level 7 using db7 mother wavelet.

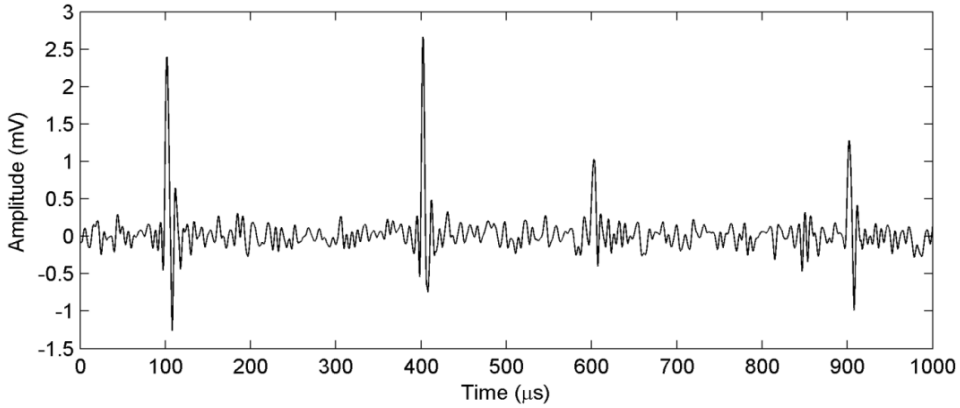

Figure 3.9(b) De-noised DOP type signal adopting reconstruction based thresholding on the time-domain components shown in Fig. 3.9(a).

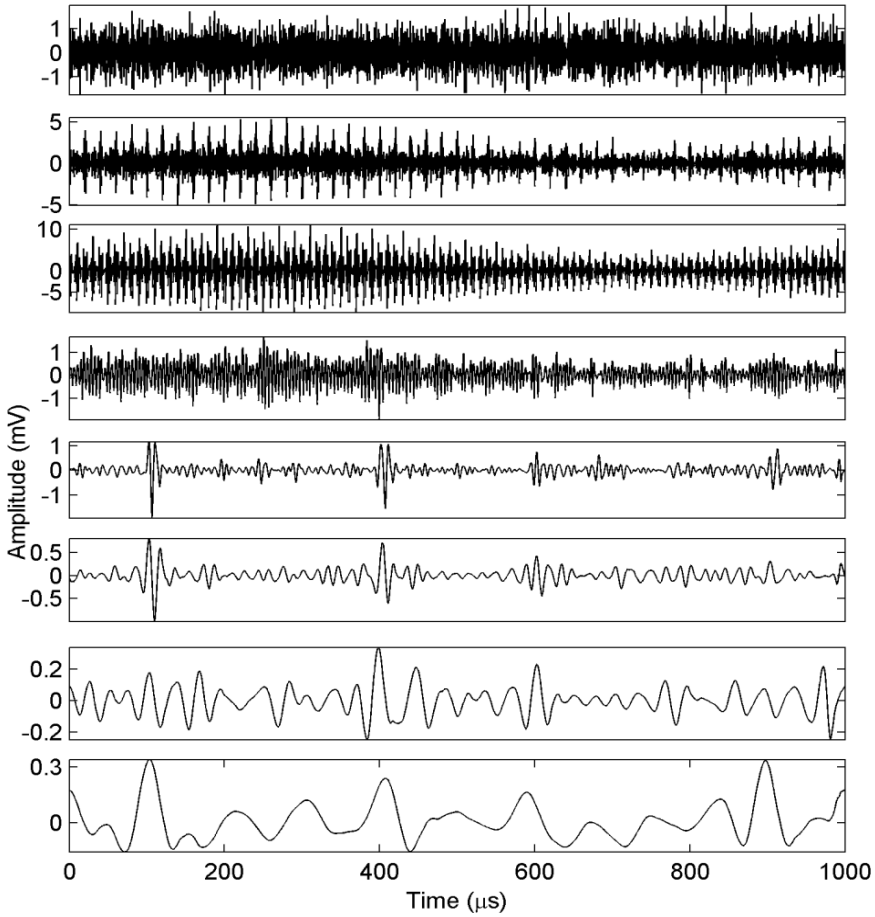

Figure 3.10(a) Reconstructed time domain components (rd1-rd7, ra7) of DOP type signal-2 DWT decomposed up to level 7 using db7 mother wavelet.

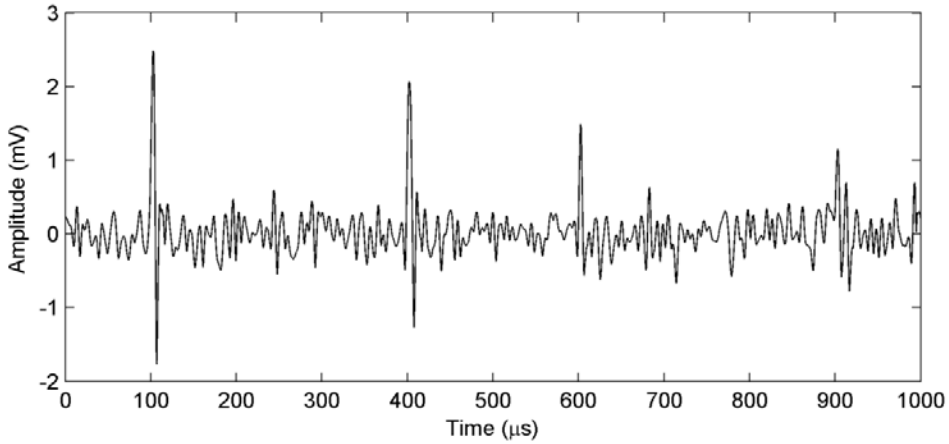

Figure 3.10(b) De-noised DOP type signal adopting reconstruction based thresholding on the time-domain components shown in Fig. 3.10(a).

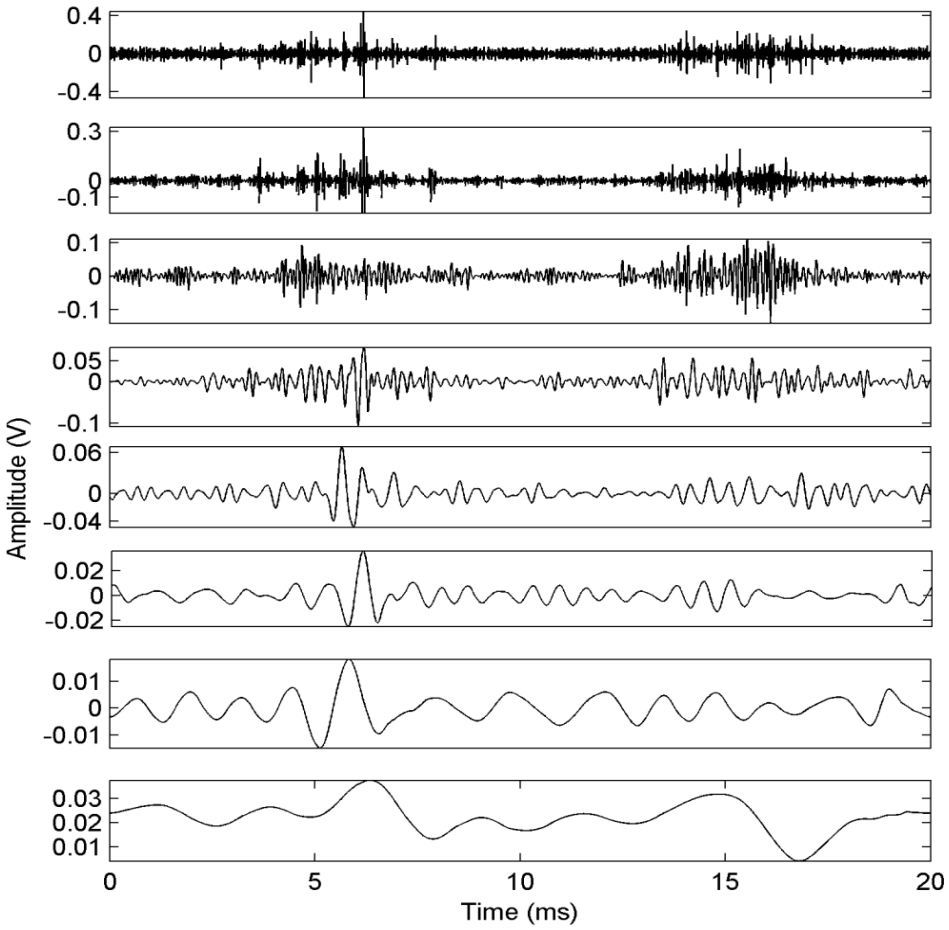

Figure 3.11(a) Reconstructed time domain components (rd1-rd7, ra7) of the practical signal DWT decomposed up to level 7 using db7 mother wavelet.

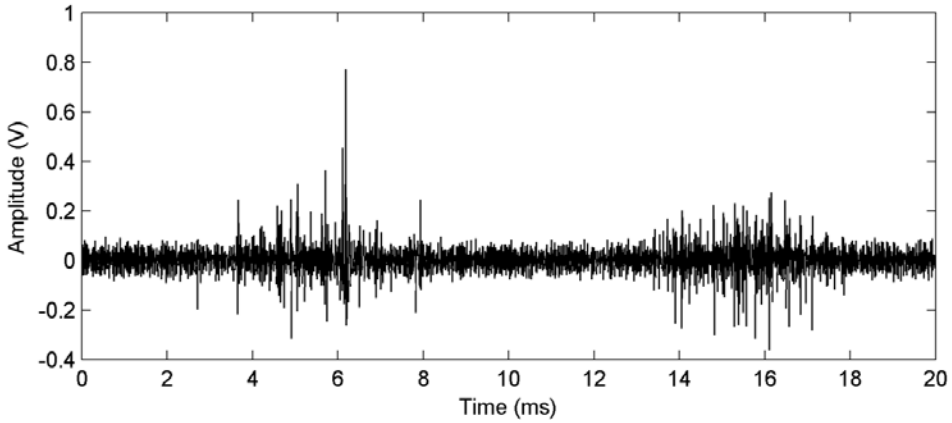

Figure 3.11(b) De-noised practical signal adopting reconstruction based thresholding on the time-domain components shown in Fig. 3.11(a).

3.6.1.3 Thresholding based on visual inspection of the DWT coefficients

In this method the threshold values are decided by visual inspection of the reconstructed components. This method is different from the reconstruction based thresholding in the respect that the reconstructed components are not added directly. But the coefficients corresponding to the components representing the signal are thresholded again. The de-noising results using this thresholding method are shown in Figs. 3.12-3.16. It is seen that the four pulses of all the simulated signals are recovered adopting this method.

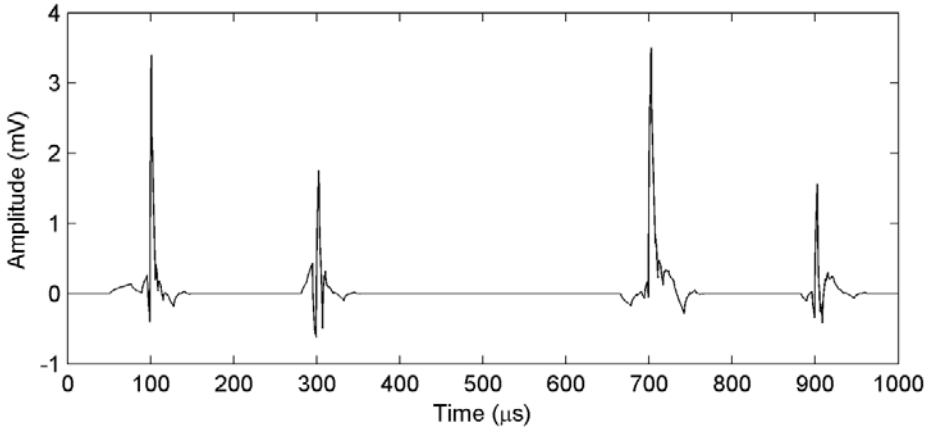

Figure 3.12. De-noising result of DEP type signal-1 using DWT based de-noising method adopting db2 as the mother wavelet, maximum decomposition level 7, and visual inspection based thresholding.

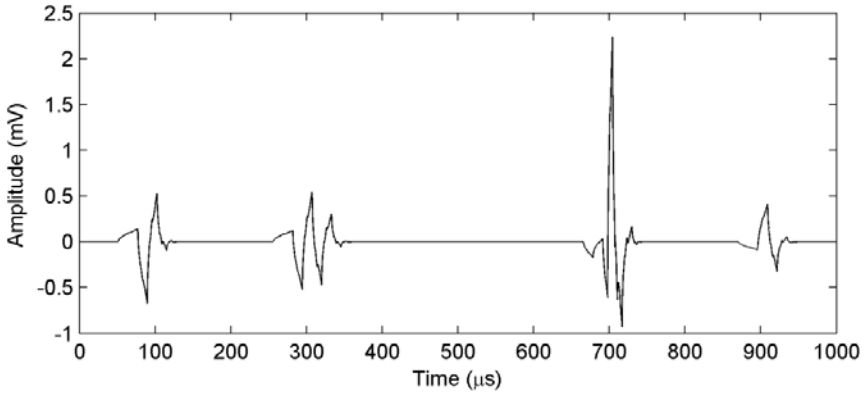

Figure 3.13. De-noising result of DEP type signal-2 using DWT based de-noising method adopting db2 mother wavelet, maximum decomposition level 7 and visual inspection based thresholding.

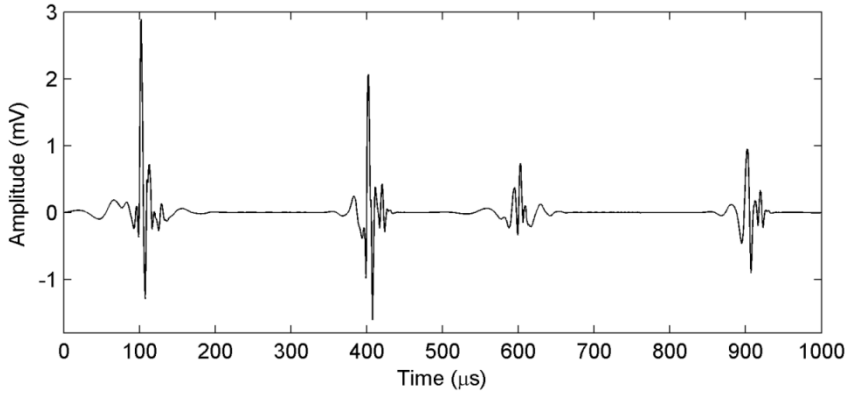

Figure 3.14. De-noising result of DOP type signal-1 using DWT based de-noising method, db7 mother wavelet, maximum decomposition level 7 and visual inspection based thresholding.

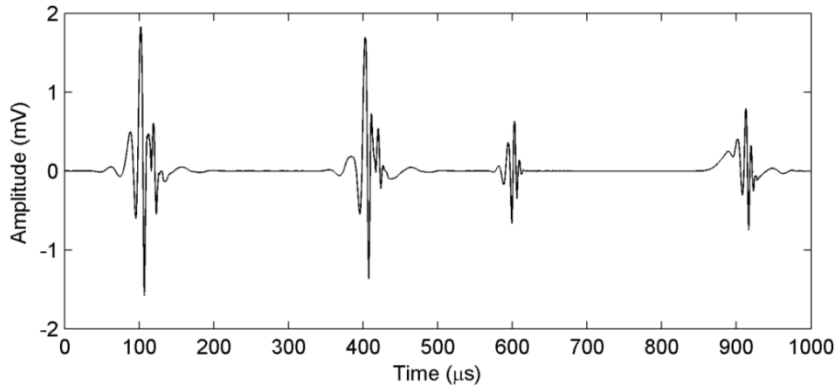

Figure 3.15. De-noising result of DOP type signal-2 using DWT based de-noising method adopting db7 mother wavelet, maximum decomposition level 7 and visual inspection based thresholding.

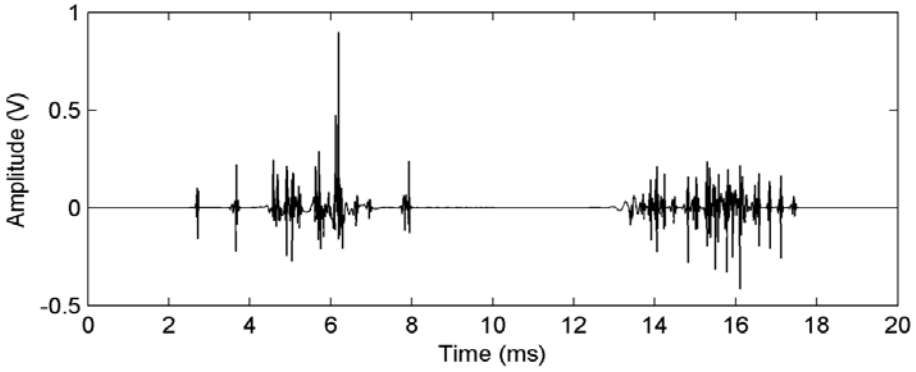

Figure 3.16. De-noising result of the practical signal using DWT based de-noising method adopting db7 mother wavelet, maximum decomposition level 7 and visual inspection based thresholding.

3.6.2 Decomposition level dependent mother wavelet selection

As mentioned earlier, scale dependent mother wavelet selection can be adopted for DWT based de-noising of PD signal. For implementing the method the energy percentage formula mentioned in (10) is used. For each level, one level DWT decomposition of the previous level approximation is carried out using different wavelets. The wavelet that generates maximum percentage of approximation energy according to (10) is selected as mother wavelet for that particular level. Using the scheme the level dependent mother wavelets for the five signals are shown in Table 3.1. For the convenience of comparison between DWT based de-noising and SGWT based de-noising, the wavelet library in this method includes only the Daubechies wavelets of order 1 to 8. Two thresholding methods are applied in this category, the automatic thresholding rule, and the visual inspection based thresholding. The reconstruction based thresholding is not applied here because all the levels are decomposed by different wavelets; hence determining the reconstructed components is difficult.

TABLE 3.1

SCALE DEPENDENT MOTHER WAVELETS FOR DIFFERENT PD SIGNALS

Signal type	level 1	level 2	level 3	level 4	level 5	level 6	level 7
DEP type signal-1	db2	db3	db7	db6	db1	db3	db2
DEP type signal-2	db8	db1	db1	db8	db8	db8	db8
DOP type signal-1	db5	db5	db5	db8	db3	db6	db5
DOP type signal-2	db8	db8	db1	db8	db8	db6	db8
Practical signal	db1	db4	db3	db6	db7	db8	db8

3.6.2.1 Automatic thresholding rule

Using the scale dependent wavelet selection method and automatic thresholding rule the DWT based de-noised signals are shown in Figs. 3.17-3.21. The de-noising results of DEP type signal-1 in Fig. 3.17 and DOP signal-1 in Fig. 3.19 show that along with the four PD pulses recovered, an extra pulse is generated. The DEP type signal-2 and DOP type signal-2 could not be de-noised using this method. The practical signal is however extracted using this method.

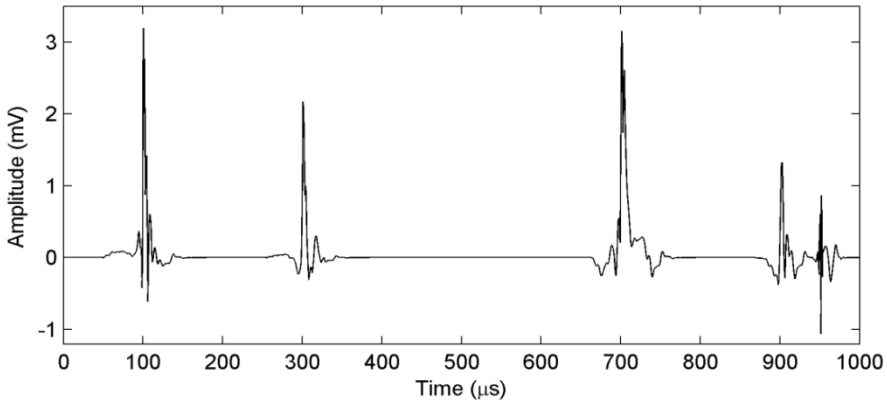

Figure 3.17. De-noising result of the DEP type signal-1 using DWT based de-noising method adopting level dependent mother wavelet selection, maximum decomposition level 7 and applying automatic thresholding rule.

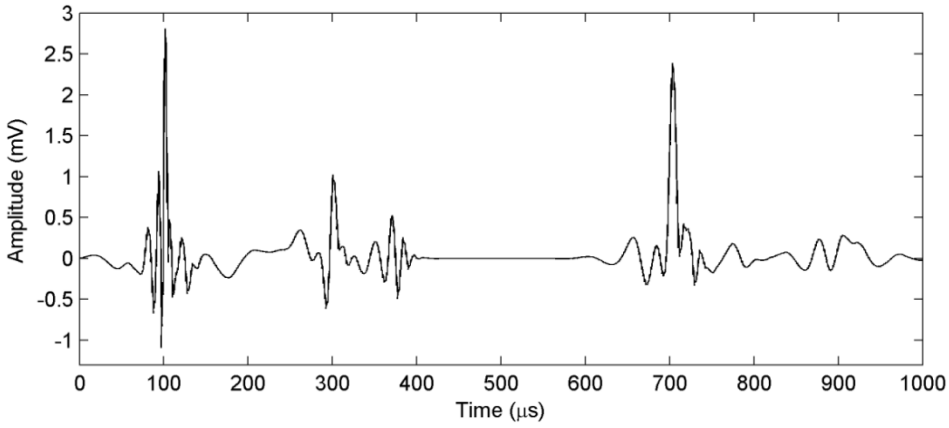

Figure 3.18. De-noising result of the DEP type signal-2 using DWT based de-noising method adopting level dependent mother wavelet selection, maximum decomposition level 7 and applying automatic thresholding rule.

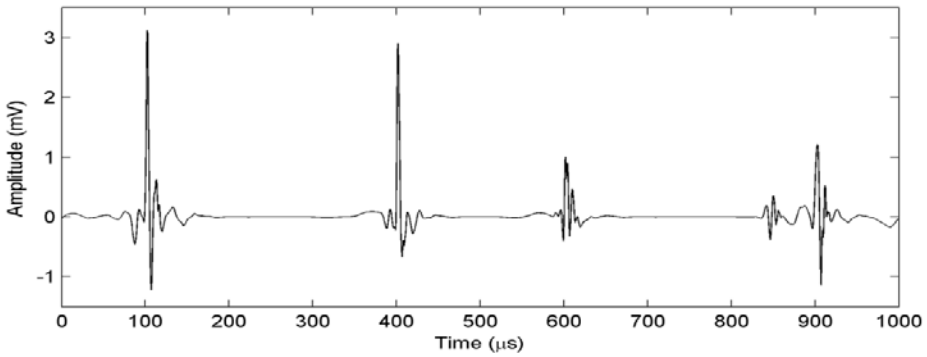

Figure 3.19. De-noising result of the DOP type signal-1 using DWT based de-noising method adopting level dependent mother wavelet selection, maximum decomposition level 7 and applying automatic thresholding rule.

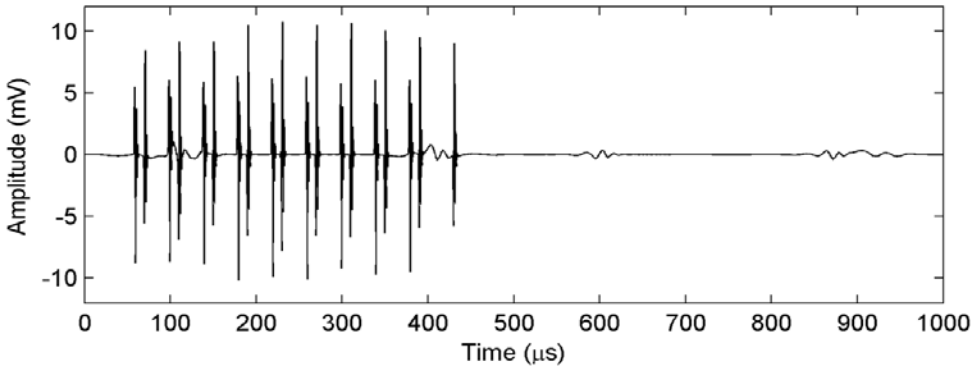

Figure 3.20. De-noising result of the DOP type signal-2 using DWT based de-noising method adopting level dependent mother wavelet selection, maximum decomposition level 7 and applying automatic thresholding rule.

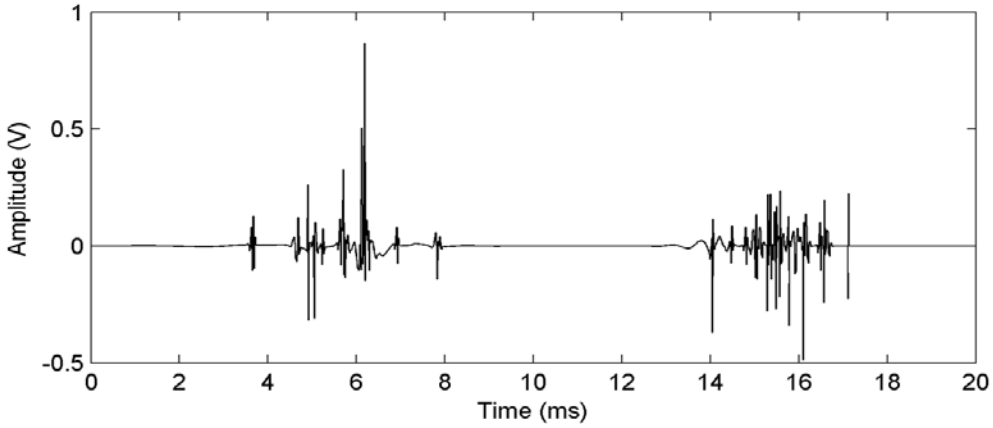

Figure 3.21. De-noising result of the practical signal using DWT based de-noising method adopting level dependent mother wavelet selection, maximum decomposition level 7 and applying automatic thresholding rule.

3.6.2.2 Thresholding based on visual inspection of the DWT coefficients

In this DWT based de-noising scheme, scale dependent mother wavelet selection method and visual inspection based thresholding is adopted. The de-noised signals adopting this method are shown in Figs. 3.22-3.26. It is seen from the figures that except DEP type signal-2 all the signals are extracted. Only two pulses of the DEP type signal-2 are recovered using this method.

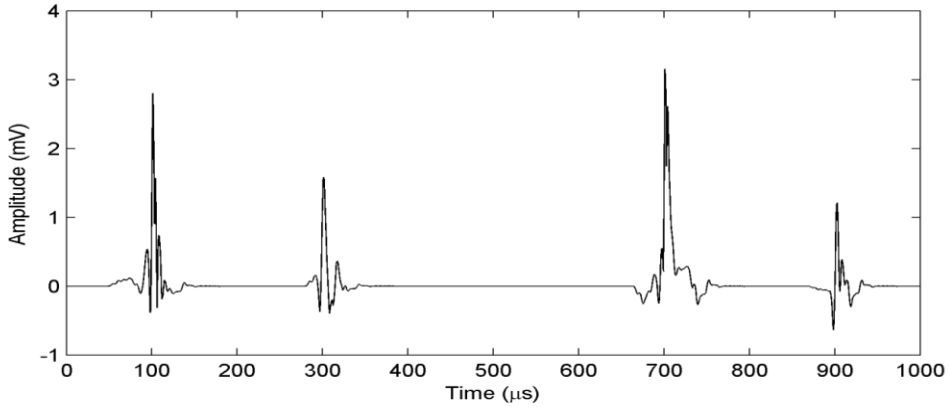

Figure 3.22. De-noising result of the DEP type signal-1 using DWT based de-noising method adopting level dependent mother wavelet selection, maximum decomposition level 7 and applying visual inspection based thresholding.

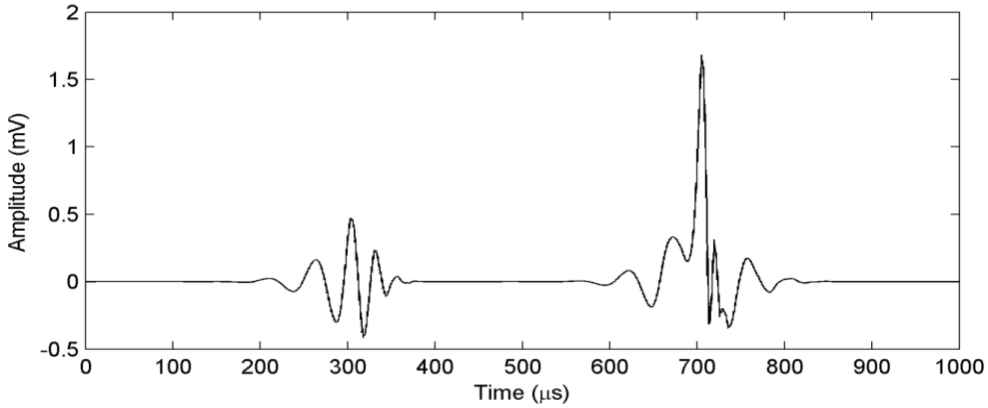

Figure 3.23. De-noising result of the DEP type signal-2 using DWT based de-noising method adopting level dependent mother wavelet selection, maximum decomposition level 7 and applying visual inspection based thresholding.

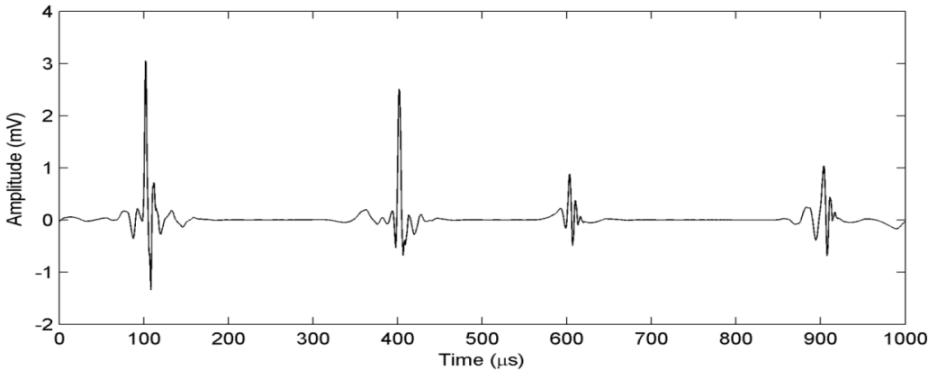

Figure 3.24. De-noising result of the DOP type signal-1 using DWT based de-noising method adopting level dependent mother wavelet selection, maximum decomposition level 7 and applying visual inspection based thresholding.

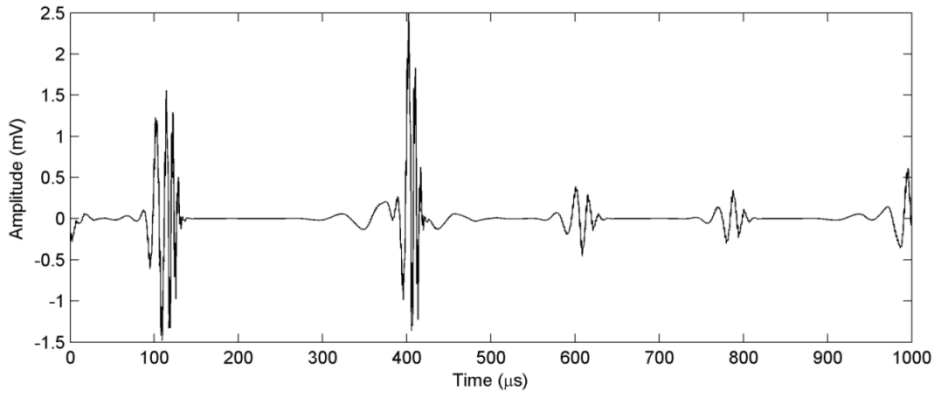

Figure 3.25. De-noising result of the DOP type signal-2 using DWT based de-noising method adopting level dependent mother wavelet selection, maximum decomposition level 7 and applying visual inspection based thresholding.

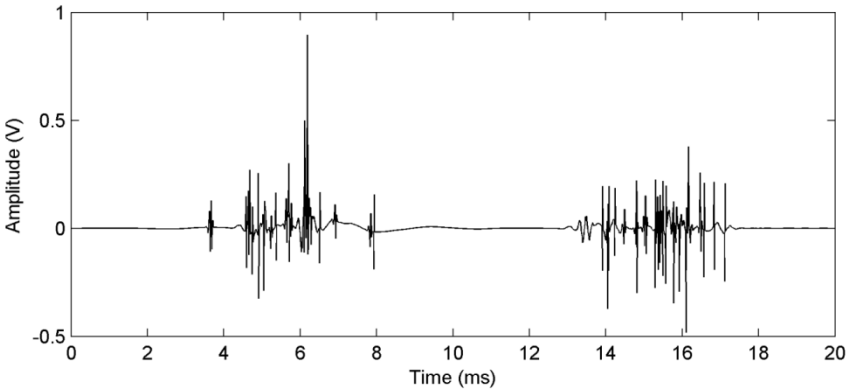

Figure 3.26. De-noising result of the practical signal using DWT based de-noising method adopting level dependent mother wavelet selection, maximum decomposition level 7 and applying visual inspection based thresholding.

3.7 Summary

Discrete wavelet transform is an effective de-noising technique for PD signals. DWT of a signal is carried out using various techniques depending on the methods of mother wavelet selection, thresholding rule and the maximum decomposition level. The de-noising method to be applied on a noisy signal depends on the kind the PD pulse to be extracted and severity of noise and interference. It is seen that for excessively noisy signal reconstruction based thresholding produce better result than automatic thresholding rule. And when both the methods fail, visual inspection based thresholding can de-noise a PD signal.

Chapter 4
De-noising of PD Signals using Second Generation Wavelet Transform

4.1 Introduction

Discrete wavelet transform (DWT) performs the wavelet analysis of a signal in frequency domain using a mother wavelet selected from the wavelet library. Though DWT is a powerful tool in de-noising noisy PD signals, it fails in severe noise conditions. Recent research shows that second generation wavelet transform (SGWT) can be employed as an alternative for the de-noising of a noisy signal. SGWT is a time domain equivalent of the DWT. It uses the lifting scheme associated with a mother wavelet to decompose the signal in to SGWT coefficients at various levels. SGWT (also called lifting wavelet transform (LWT)) shows more accuracy in PD signal de-noising, if the shape of the PD pulse to be extracted is known before. Using the information, the wavelet filters can be modified to suit the requirements and the de-noising results using the lifting scheme of the modified wavelet filters gives more accuracy. The SGWT allows for an in-place implementation of the DWT. It means that the DWT can be implemented without allocating auxiliary memory and hence SGWT decreases the hardware requirements while improving the speed of calculation [9].

4.2 Second generation wavelet transform (SGWT)

SGWT is a time domain construction of bi-orthogonal wavelets based on the process known as lifting scheme (LS) [9]. SGWT provides an entirely time-domain interpretation of the transform as opposed to frequency domain based approach by conventional wavelet transform (WT). Application of SGWT is not confined to designing wavelets and performing the DWT, the associated LS makes it more flexible, maintaining reversibility, and so SGWT can be employed for PD de-noising. The LS in SGWT is shown in Figs. 4.1(a) and 4.1(b), which consists of iteration of three basic operations: split, predict and update [9].

4.2.1 Split

In this step the original signal $S[n]$ is divided into two disjoint subsets, $X[n] = S_{even}[n]$ the even indexed points, and $Y[n] = S_{odd}[n]$, the odd indexed points. The even and odd sequences are

highly correlated. This local similarity feature of the original signal makes it possible to predict and update as mentioned below.

4.2.2 Predict

This step determines the detail coefficients $d[n]$ of the original signal $S[n]$ in the wavelet decomposition using (19). Using the prediction operator P, $Y[n]$ is predicted from $X[n]$.

$$d[n] = Y[n] - P(X[n]) \tag{19}$$

4.2.3 Update

This step determines the approximation coefficients $c[n]$ of the original signal $S[n]$ using (20). To obtain $c[n]$, an update operator U is applied on the detail coefficients and the result is added to the $X[n]$.

$$c[n] = X[n] + U(d[n]) \tag{20}$$

The approximation generated at the first level is made to repeat the above three steps again and so on. Fig. 4.1(b) shows the inverse LS. The original signal can be perfectly reconstructed adopting inverse second generation wavelet transform (ISGWT) [9].

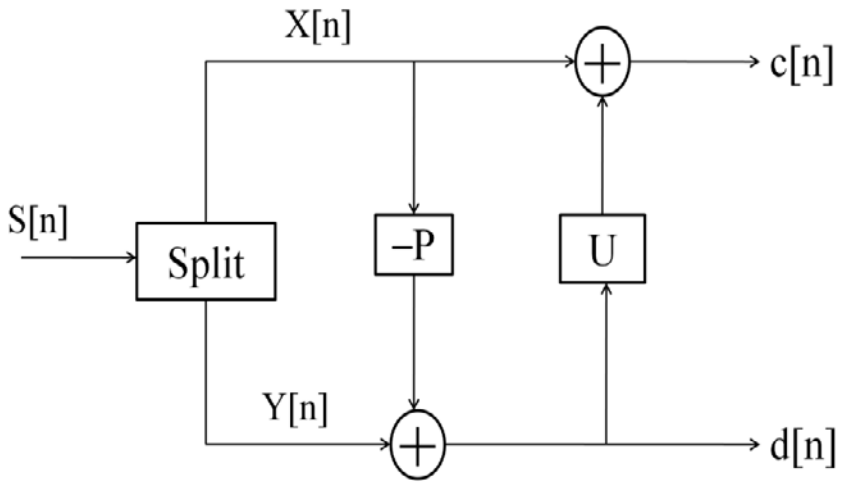

Figure 4.1(a) Block diagram of second generation wavelet transform decomposition.

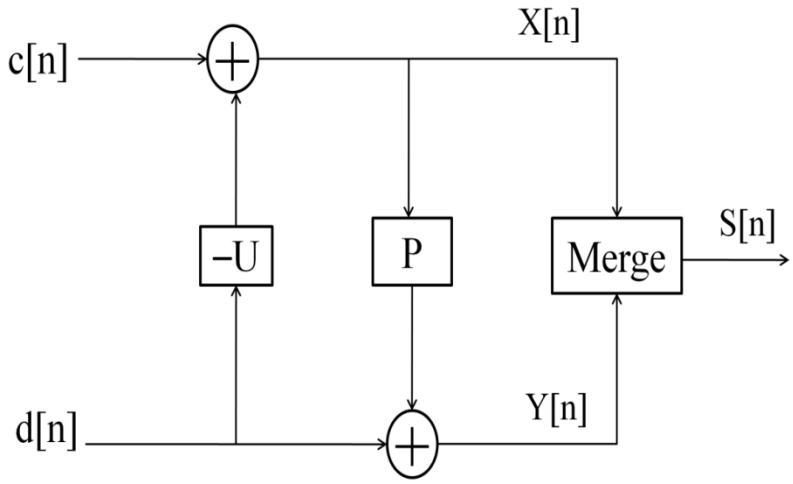

Figure 4.1(b) Block diagram of second generation wavelet transform reconstruction.

4.3 De-noising of PD signals using SGWT

Second generation wavelet transform based de-noising of PD signal starts with choosing a suitable mother wavelet. The lifting scheme associated with the mother wavelet is used for lifting wavelet decomposition of the signal up to a particular level. Then the highest level approximation coefficients and detail coefficients of all levels are soft or hard thresholded adopting a thresholding rule. Finally the de-noised signal is reconstructed using ISGWT of the modified approximation and detail coefficients. The proposed SGWT based de-noising method is implemented using MATLAB toolbox. The implementation of PD signal de-noising method using SGWT is similar to the DWT. The rules for SGWT based de-noising, like mother wavelet selection, choosing maximum decomposition level, thresholding rule determination are similar to the DWT based de-noising method. The SGWT (or LWT) based de-noising results of the five signals are given below.

4.3.1 Level independent mother wavelet selection

In SGWT the level independent mother wavelet selection method adopts the similar, method as in DWT. Here also for DEP type pulse extraction db2 mother wavelet is employed and for DOP type pulse extraction db7 mother wavelet is used. For the practical PD signal de-noising, db7 wavelet is chosen randomly. SGWT is a time domain representation of wavelet transform and unless the wavelet filters are modified, there will not be any appreciable change in the de-noising results. Hence automatic thresholding rule is not applied here to the excessively noisy

signals DEP type signal-2 and DOP type signal-2. And as the automatic thresholding rule shows appreciable results for the other three signals they are de-noised by automatic thresholding rule. However the visual inspection based thresholding is not applied to them here. Also two thresholding methods are employed here, automatic thresholding rule and visual inspection based thresholding.

4.3.1.1 Automatic thresholding rule

Figs. 4.2-4.4 show the LWT based de-noising results adopting level independent mother wavelet selection and automatic thresholding rule. It is seen that in the de-noised DEP type signal-1, one more pulse appears. However DOP type signal-1 could be extracted. The de-noised practical signal is shown in Fig. 4.4.

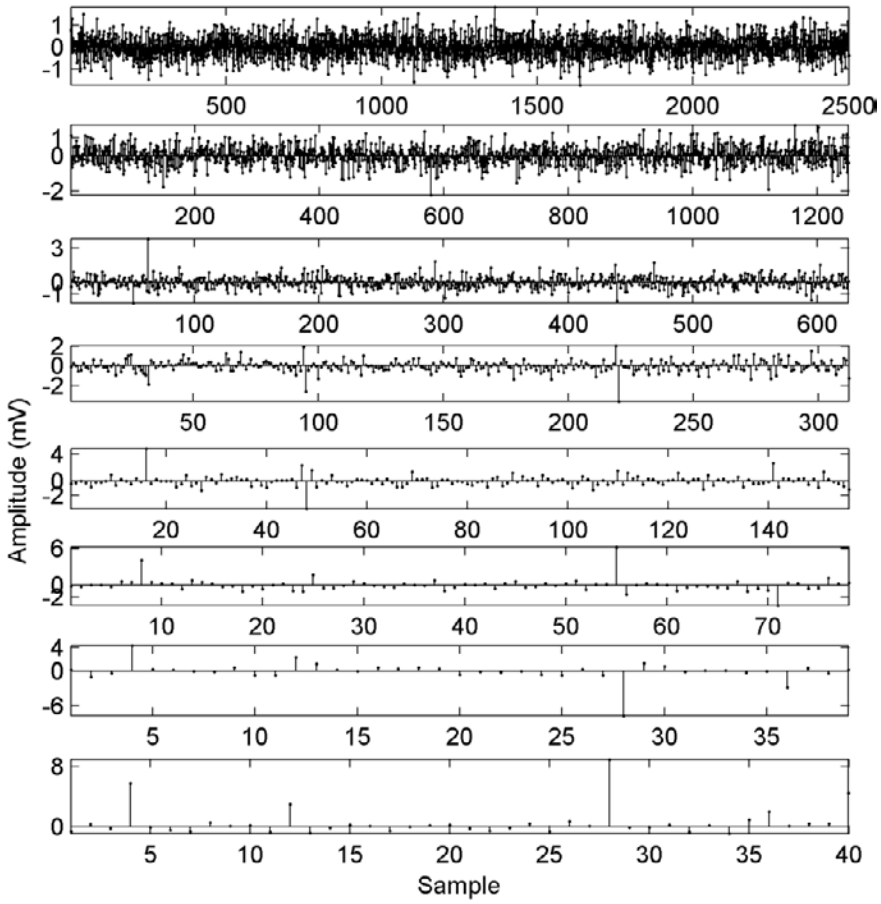

Figure 4.2(a) LWT coefficients (d1-d7, a7) of the DEP type signal-1 decomposed up to level 7 using db2 wavelet based lifting scheme.

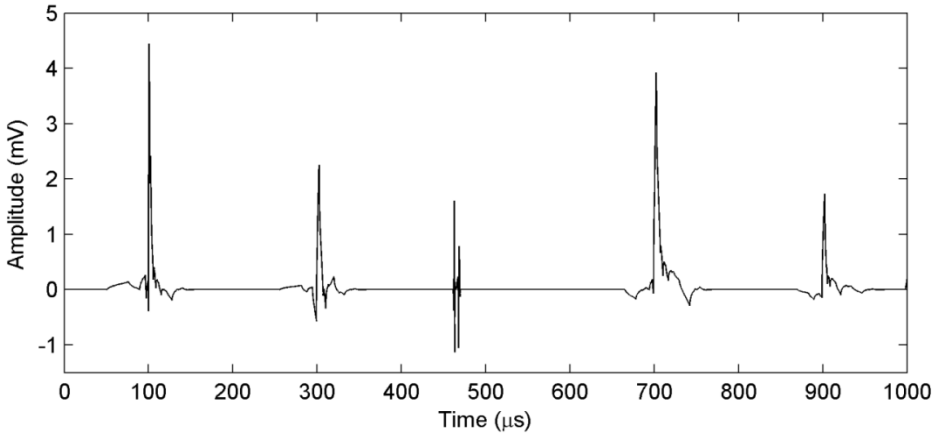

Figure 4.2(b) De-noised DEP type signal adopting automatic thresholding rule on the coefficients shown in Fig. 4.2(a).

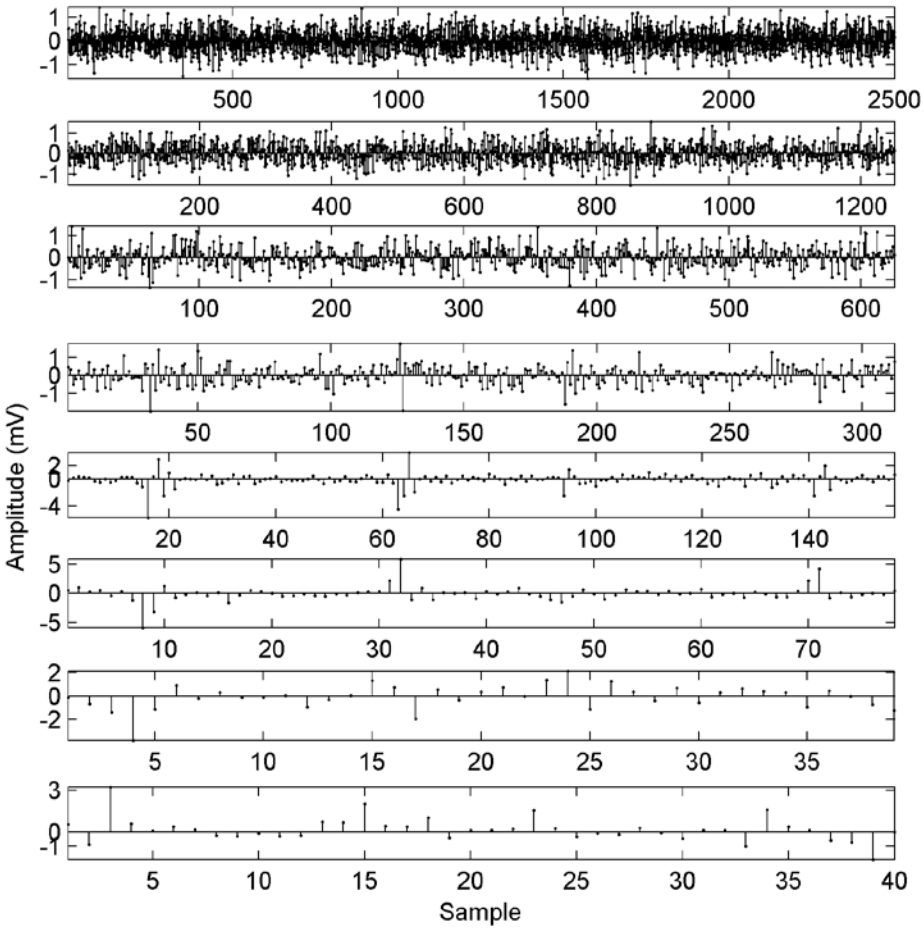

Figure 4.3(a) LWT coefficients (d1-d7, a7) of the DOP type signal-1 decomposed up to level 7 using db7 wavelet based lifting scheme.

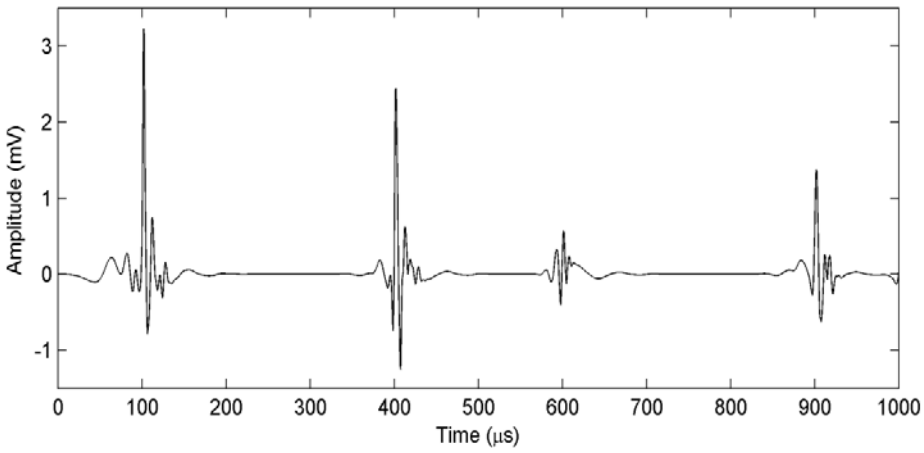

Figure 4.3(b) De-noised DOP type signal adopting automatic thresholding rule on the coefficients shown in Fig. 4.3(a).

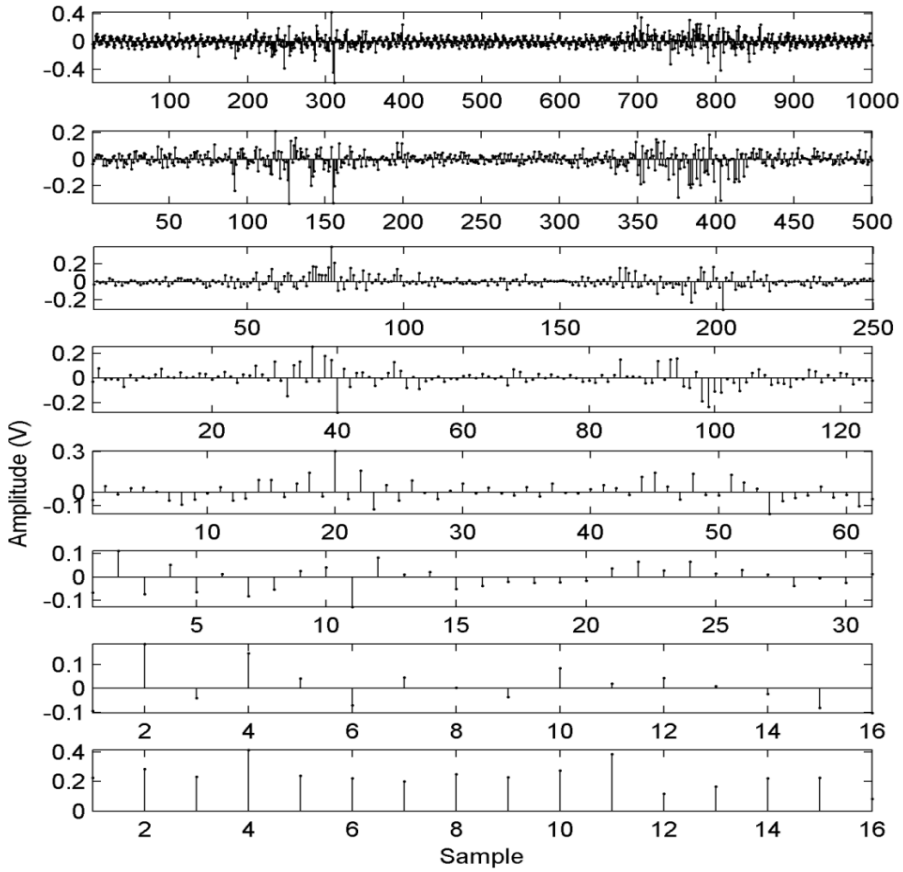

Figure 4.4(a) LWT coefficients (d1-d7, a7) of the practical signal decomposed up to level 7 using db7 wavelet based lifting scheme.

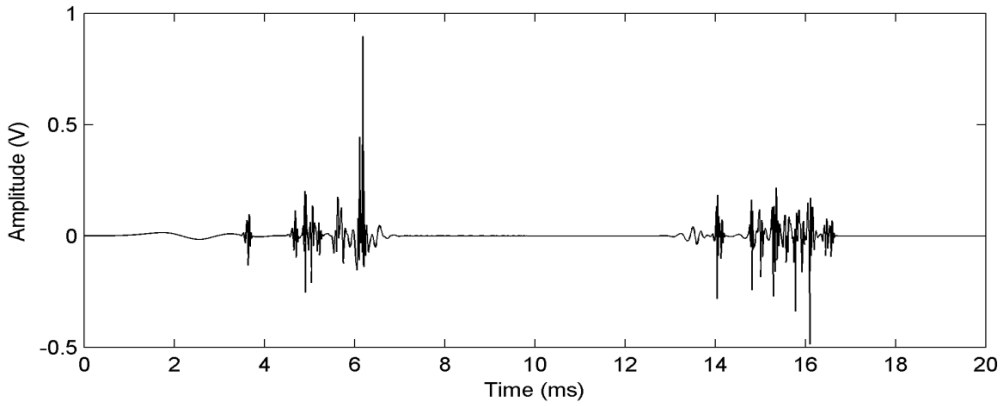

Figure 4.4(b) De-noised practical signal adopting automatic thresholding rule on the coefficients shown in Fig. 4.4(a).

4.3.1.2 Visual inspection based thresholding

In this method of LWT based PD signal de-noising, level independent mother wavelet selection method and visual inspection based thresholding are employed. The de-noising results are shown in Figs. 4.5 and 4.6. It is seen that the pulses of both DEP type signal-2 and DOP type signal-2 are recovered in this method.

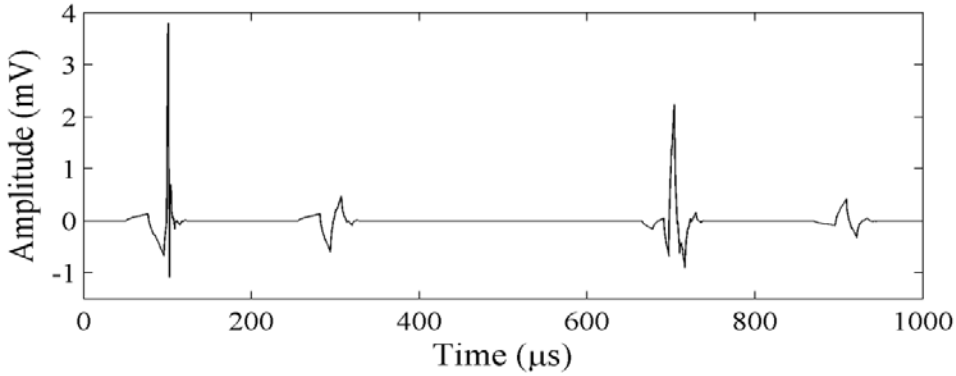

Figure 4.5. De-noising result of the DEP type signal-2 using LWT based de-noising method adopting db2 wavelet based lifting scheme, maximum decomposition level 7 and applying visual inspection based thresholding.

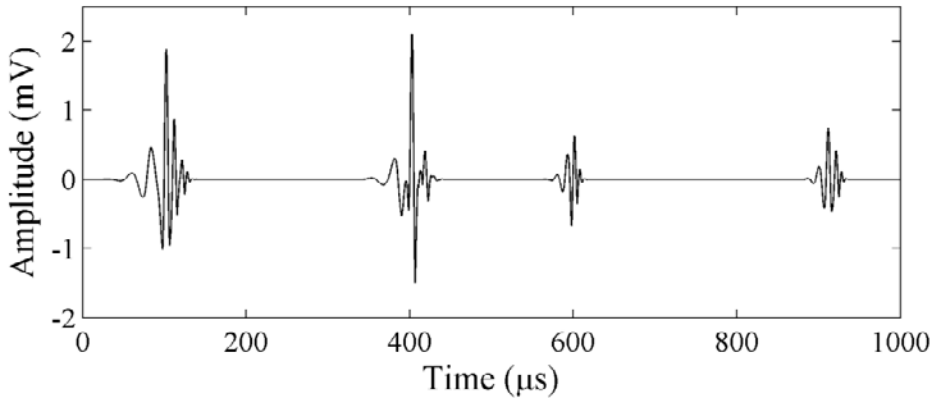

Figure 4.6. De-noising result of the DOP type signal-2 using LWT based de-noising method adopting db7 wavelet based lifting scheme, maximum decomposition level 7 and applying visual inspection based thresholding.

4.3.2 Level dependent mother wavelet selection

In this LWT based de-noising method the wavelets for different levels are chosen according to the maximum approximation energy criterion mentioned before. The mother wavelets chosen here for the different levels are same as in DWT. As the scale dependent mother wavelet selection does not produce appreciable results in DWT only automatic thresholding rule is applied here to the DEP type signal-1, DOP type signal-1 and the practical signal. The other two signals are excluded as they could not be de-noised using this thresholding rule in DWT.

4.3.2.1 Automatic thresholding rule

In this LWT based de-noising method, level dependent mother wavelet selection and automatic thresholding rule is employed. The de-noising results are shown in Figs. 4.7-4.9. Fig. 4.7 shows that the de-noised DEP type signal-1 contains one extra pulse. However the DOP type signal-1 is extracted using this method.

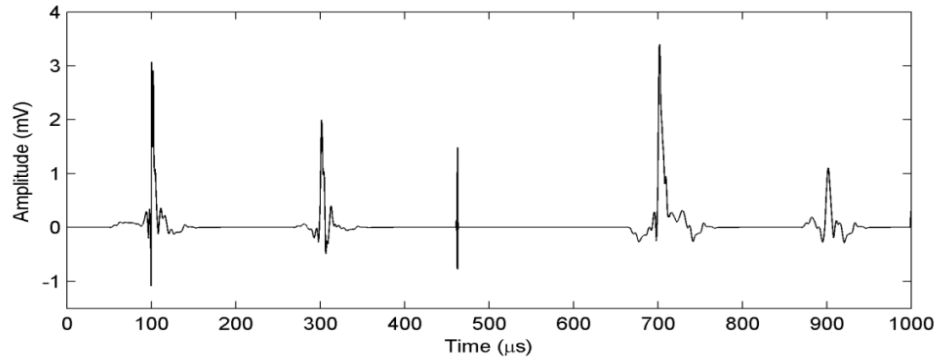

Figure 4.7. De-noising result of the DEP type signal-1 using LWT based de-noising method adopting level dependent mother wavelet selection, maximum decomposition level 7 and applying automatic thresholding rule.

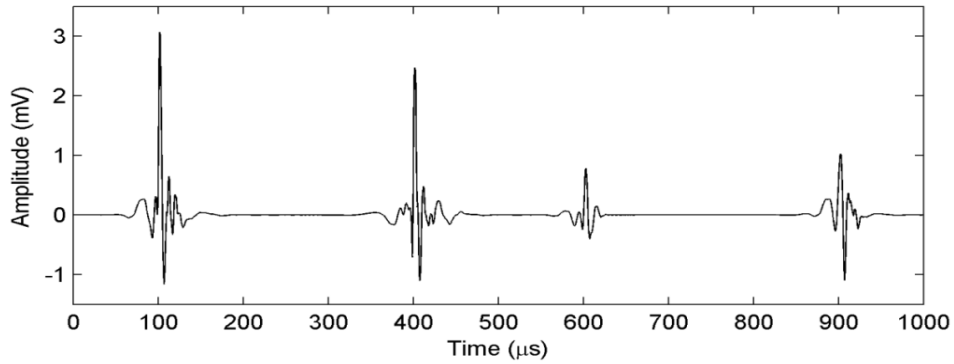

Figure 4.8. De-noising result of the DOP type signal-1 using LWT based de-noising method adopting level dependent mother wavelet selection, maximum decomposition level 7 and applying automatic thresholding rule.

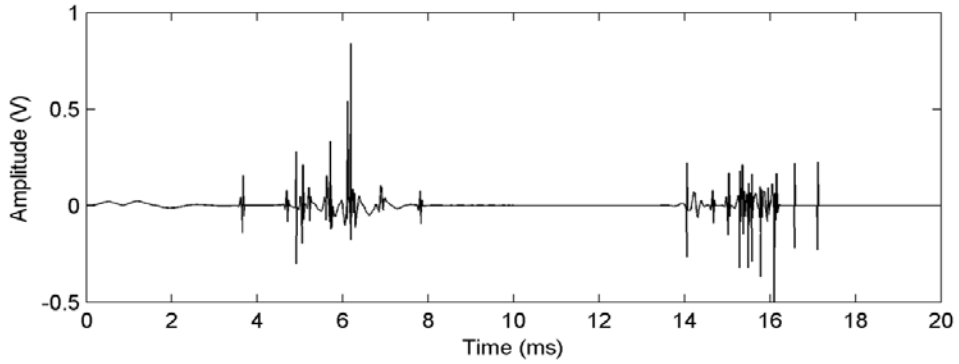

Figure 4.9. De-noising result of the practical signal using LWT based de-noising method adopting level dependent mother wavelet selection, maximum decomposition level 7 and applying automatic thresholding rule.

4.4 Comparison between the de-noising techniques adopted

Tables 4.1-4.5 compare the different de-noising techniques applied to the five signals mentioned earlier in this thesis. In the tables only successful de-noising techniques are compared. An effective de-noising method requires low amplitude error (AE), low mean square error (MSE) and high SNR. Table 1 compares the de-noising techniques applied to the DEP type signal-1 which is generated by adding WGN at SNR -5dB to the clean DEP type signal. It is found in Table 1 that DWT based de-noising method, adopting level independent mother wavelet and automatic thresholding rule produces better de-noising result as compared to other methods. It is also seen that reconstruction based thresholding is not suitable for less noisy signals. For de-noising PD signals with SNR more than -5 dB, automatic thresholding rule gives better results.

Table 4.2 compares the de-noising techniques applied to DEP type signal-2 obtained by corrupting a clean DEP type signal by WGN at SNR -10 dB and DSIs. It is found that only three methods de-noised the PD signal. The de-noised signals are however too much attenuated and distorted. The de-noising results by all the three methods are almost similar. In terms of SNR and MSE, the LWT based, level independent mother wavelet selection method and visual inspection based thresholding produces better de-noising result.

Table 4.3 evaluates the various de-noising techniques applied to DOP type signal-1. It is found that the DWT based de-noising using level dependent mother wavelet selection and automatic thresholding rule produces the best de-noising result for DOP type signal-1.

Table 4.4 compares the de-noising techniques applied to the DOP type signal-2. Among the three techniques mentioned, DWT based level independent mother wavelet selection and reconstruction based thresholding produces good result if amplitude of the pulses is the main concern. Otherwise any of the other two methods produces better SNR and low MSE.

Table 4.5 evaluates the de-noising techniques applied to a practical PD signals. In case of practical PD signal there is no reference PD signal. Hence unlike simulated signals here the de-noising performance is measured using reduction in noise level. It is found that the LWT based de-noising methods remove more noise than the DWT based methods. Also the LWT based de-noising methods require less time for the de-noising than the DWT based methods. For the practical signal, the LWT based de-noising method adopting level independent mother wavelet selection and automatic thresholding rule, produces the best result.

TABLE 4.1
COMPARISON OF DIFFERENT WAVELET BASED DE-NOISING TECHNIQUES APPLIED TO DEP TYPE SIGNAL-1 (DEP TYPE SIGNAL NOISED BY WGN AT SNR -5dB)

De-noising technique	Pulse no.	AE (%)	SNR (dB)	MSE (10^{-8})
DWT, level dependent wavelet selection, automatic thresholding	Pulse1	20.16	7.46	1.4758
	Pulse2	7.94		
	Pulse3	4.28		
	Pulse4	18.61		
DWT, level dependent wavelet selection, visual inspection based thresholding	Pulse1	29.91	6.789	1.72
	Pulse2	32.89		
	Pulse3	4.28		
	Pulse4	25.8		
DWT, level independent mother wavelet selection, automatic thresholding	Pulse1	7.246	9.17	0.993
	Pulse2	14.68		
	Pulse3	-0.21		
	Pulse4	-17.199		
DWT, level independent mother wavelet selection, visual inspection based thresholding	Pulse1	15.14	7.71	1.39
	Pulse2	25.38		
	Pulse3	-6.28		
	Pulse4	4.36		
DWT, level independent mother wavelet selection, reconstruction based thresholding	Pulse1	25.91	4.23	3.099
	Pulse2	33.19		
	Pulse3	12.90		
	Pulse4	-19.10		
LWT, level dependent wavelet selection, automatic thresholding	Pulse1	23.16	8.38	1.19
	Pulse2	15.15		
	Pulse3	-3.22		
	Pulse4	32.37		
LWT, level independent mother wavelet selection, automatic thresholding	Pulse1	-11.09	8.71	1.105
	Pulse2	4.41		
	Pulse3	-19.12		
	Pulse4	-6.39		

TABLE 4.2
COMPARISON OF DIFFERENT WAVELET BASED DE-NOISING TECHNIQUES APPLIED TO DEP TYPE SIGNAL-2 (DEP TYPE SIGNAL NOISED BY WGN AT SNR -10dB AND DSI)

De-noising technique	Pulse no.	AE (%)	SNR (dB)	MSE (10^{-8})
DWT, level independent mother wavelet selection, visual inspection based thresholding	Pulse1	86.83	1.61	5.66
	Pulse2	77.088		
	Pulse3	31.93		
	Pulse4	75.04		
DWT, level independent mother wavelet selection, reconstruction based thresholding	Pulse1	54.34	1.21	6.2
	Pulse2	51.82		
	Pulse3	9.38		
	Pulse4	42.23		
LWT, level independent mother wavelet selection, visual inspection based thresholding	Pulse1	5.07	1.68	5.58
	Pulse2	79.75		
	Pulse3	32.12		
	Pulse4	74.92		

TABLE 4.3
COMPARISON OF DIFFERENT WAVELET BASED DE-NOISING TECHNIQUES APPLIED TO DOP TYPE SIGNAL-1 (DOP TYPE SIGNAL NOISED BY WGN AT SNR -5dB)

De-noising technique	Pulse no.	AE (%)	SNR (dB)	MSE (10^{-8})
DWT, level dependent wavelet selection, automatic thresholding	Pulse1	2.38	8.1	1.00
	Pulse2	-0.48		
	Pulse3	41.97		
	Pulse4	24.45		
DWT, level dependent wavelet selection, visual inspection based thresholding	Pulse1	4.39	6.69	1.38
	Pulse2	13.06		
	Pulse3	49.75		
	Pulse4	35.59		
DWT, level independent mother wavelet selection, automatic thresholding	Pulse1	10.50	7.667	1.105
	Pulse2	11.47		
	Pulse3	25.50		
	Pulse4	26.57		
DWT, level independent mother wavelet selection, visual inspection based thresholding	Pulse1	9.473	6.017	1.615
	Pulse2	28.35		
	Pulse3	57.38		
	Pulse4	41.46		
DWT, level independent mother wavelet selection, reconstruction based thresholding	Pulse1	24.84	4.890	2.094
	Pulse2	7.59		
	Pulse3	41.10		
	Pulse4	20.47		
LWT, level dependent wavelet selection, automatic thresholding	Pulse1	3.82	7.812	1.068
	Pulse2	14.38		
	Pulse3	54.57		
	Pulse4	37.08		
LWT, level independent mother wavelet selection, automatic thresholding	Pulse1	-1.223	7.017	1.283
	Pulse2	15.216		
	Pulse3	67.043		
	Pulse4	14.312		

TABLE 4.4
COMPARISON OF DIFFERENT WAVELET BASED DE-NOISING TECHNIQUES APPLIED TO DOP TYPE SIGNAL-2 (DOP TYPE SIGNAL NOISED BY WGN AT SNR -10dB AND DSI)

De-noising technique	Pulse no.	AE (%)	SNR (dB)	MSE (10^{-8})
DWT, level independent mother wavelet selection, visual inspection based thresholding	Pulse1	42.69	3.503	2.88
	Pulse2	41.28		
	Pulse3	63.51		
	Pulse4	50.78		
DWT, level independent mother wavelet selection, reconstruction based thresholding	Pulse1	22.11	1.397	4.6816
	Pulse2	29.46		
	Pulse3	13.79		
	Pulse4	28.43		
LWT, level independent mother wavelet selection, visual inspection based thresholding	Pulse1	40.90	3.32	3
	Pulse2	28.84		
	Pulse3	63.23		
	Pulse4	53.90		

TABLE 4.5
COMPARISON OF DIFFERENT WAVELET BASED DE-NOISING TECHNIQUES APPLIED TO THE PRACTICAL SIGNAL

De-noising technique	Reduction in noise level (dB)	Time taken (s)
DWT, level dependent wavelet selection, automatic thresholding	-23.69	0.1706
DWT, level dependent wavelet selection, visual inspection based thresholding	-24.27	0.1581
DWT, level independent mother wavelet selection, automatic thresholding	-23.97	0.1818
DWT, level independent mother wavelet selection, visual inspection based thresholding	-24.05	0.1671
DWT, level independent mother wavelet selection, reconstruction based thresholding	-27.93	0.1629
LWT, level dependent wavelet selection, automatic thresholding	-23.60	0.0707
LWT, level independent mother wavelet selection, automatic thresholding	-23.38	0.0673

4.5 Summary

Second generation wavelet transform employs lifting scheme of a selected wavelet to perform the decomposition of a signal up to a level generating the LWT coefficients at various levels. Then the coefficients are thresholded using the scheme as in DWT. Then inverse second generation wavelet transform is adopted for the reconstruction of the de-noised signal. In this chapter the theory of SGWT is presented. The five noisy signals are de-noised using SGWT applying the methods that successfully de-noised the signals in DWT. A comparative analysis is carried out between DWT and SGWT based de-noising results.

Chapter 5
Application of S-transform to PD Signal Analysis

5.1 The discrete S-transform

S-transform is an effective tool for time-frequency representation of signals. Let p [kT], k=0, 1, 2…., N-1 denotes a discrete time signal with a sampling time interval of T. The discrete Fourier transform of the signal is given as [12]

$$P\left[\frac{n}{NT}\right] = \frac{1}{N}\sum_{k=0}^{N-1} p[kT]e^{-(i2\pi mk/N)} \tag{21}$$

where, n = 0, 1, …., N-1. N is the length of the signal. The inverse discrete Fourier transform is

$$p[kT] = \sum_{n=0}^{N-1} P\left[\frac{n}{NT}\right]e^{i2\pi mk/N} \tag{22}$$

The S-transform of the discrete time signal p [kT], is given by [12]

$$S\left[\frac{n}{NT}, jT\right] = \sum_{m=0}^{N-1} P\left[\frac{m+n}{NT}\right]G(n,m)e^{i2\pi mj/N} \tag{23}$$

where, $G(n,m) = e^{-(2\pi^2 m^2\alpha^2/n^2)}$ is the Gaussian function [22] and where j, m, n=0, 1, N-1. Here, j is the time sample and n is the frequency sample. The factor α controls the time and frequency resolution of the transform. A lower α means higher time resolution and a higher value of α means higher frequency resolution [18].

5.2 Time-frequency representation of PD signal

Time-frequency representation (TFR) of a signal can be carried out using S-transform. The representation gives information about the frequency components and their locations in the signal. In this work the practical signal is studied using the S-transform. In Table 4.5, it is found that the LWT based de-noising scheme, using level independent mother wavelet selection method and automatic thresholding rule produces the best de-noising result for the practical signal. The de-noised practical PD signal is used here for its TFR. For low value of α the frequency resolution of the PD signal is poor, though time resolution is good. Hence, the value of α is increased from 1 to higher values to increase the frequency resolution. The TFR of the noisy practical PD signal using S-transform at α = 4 is shown in Fig. 5.1. S-transform based

TFR of the de-noised PD signal for different values of α are shown in Figs. 5.2-5.7. It is seen in the figures that, as the value of the factor α increases, the frequency resolution of the signal improves.

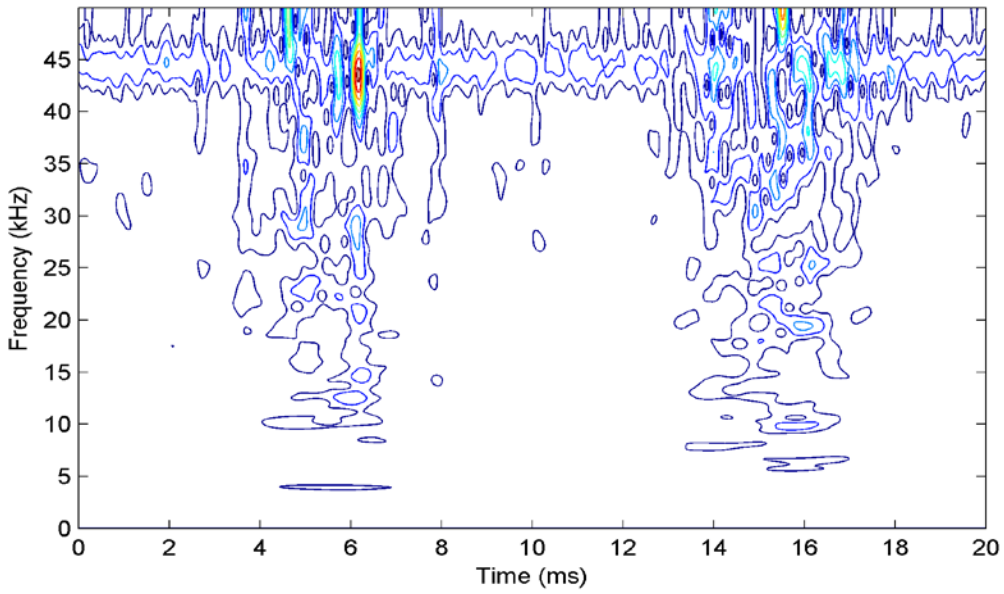

Figure 5.1. S-transform contour of the noisy practical PD signal for α =4.

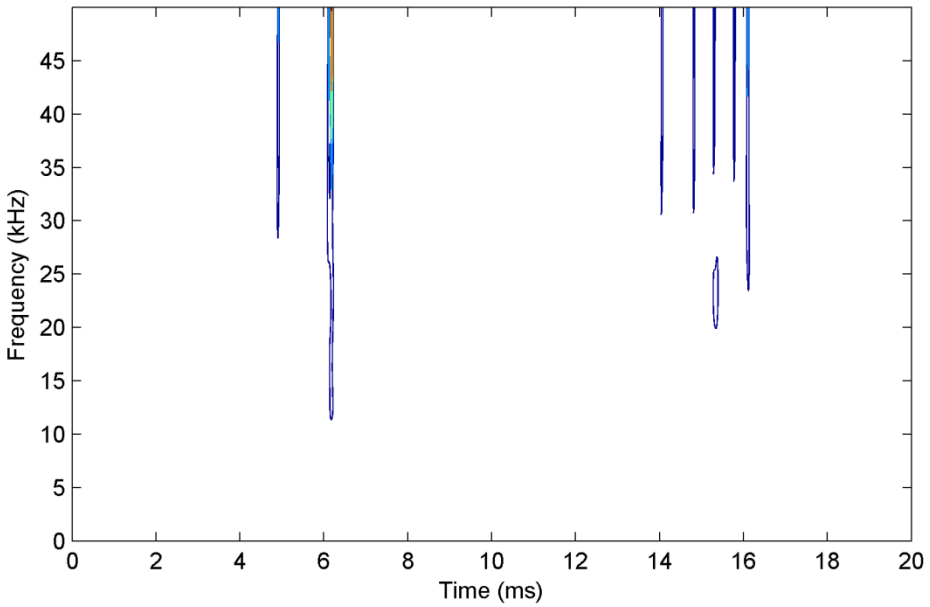

Figure 5.2. S-transform contour of the de-noised practical PD signal for α =1.

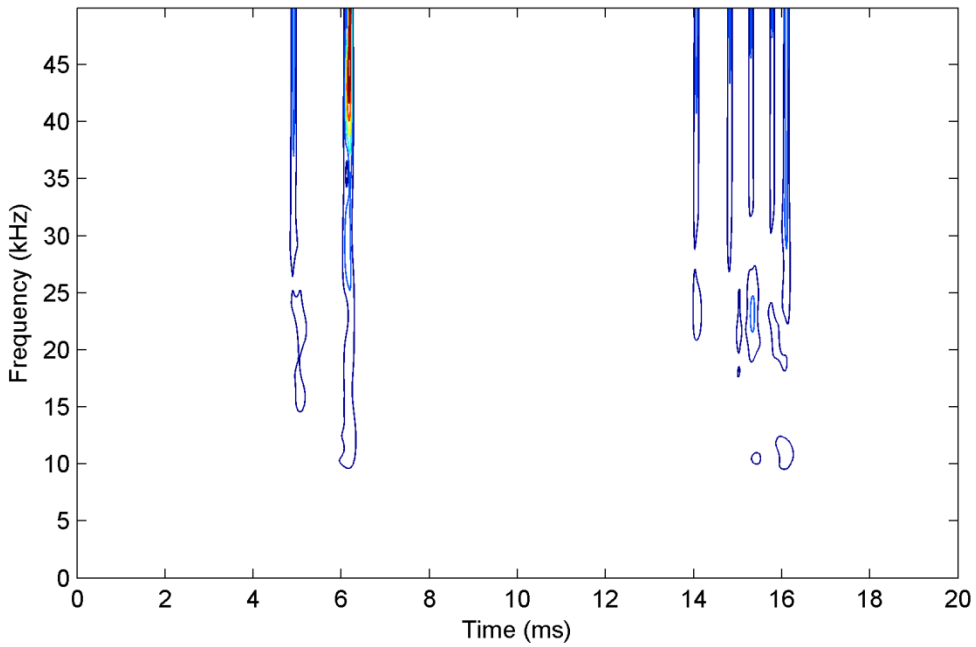

Figure 5.3. S-transform contour of the de-noised practical PD signal for α =2.

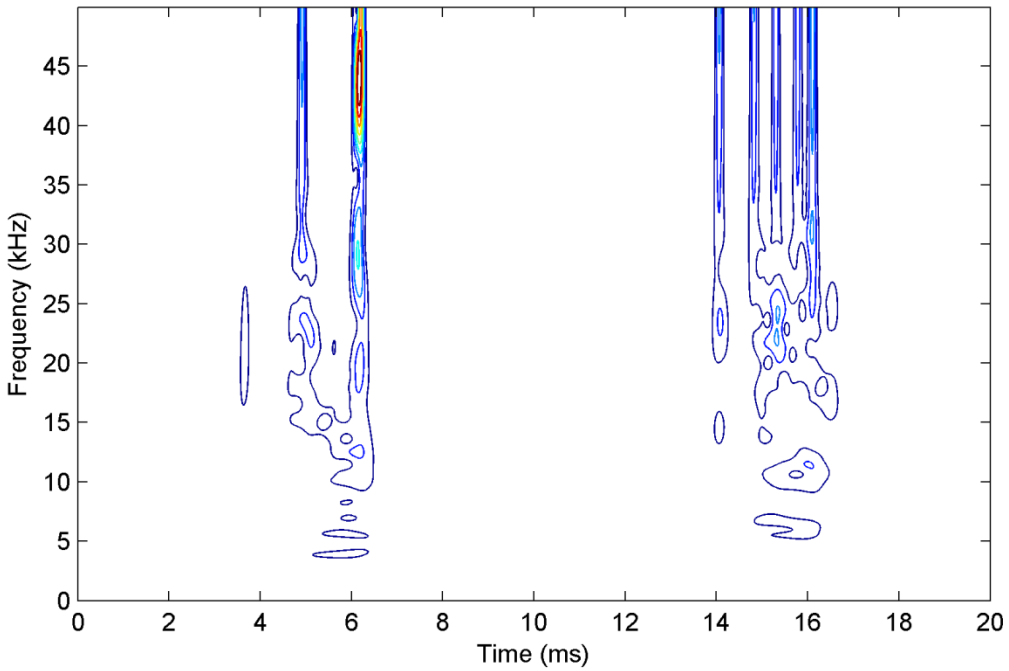

Figure 5.4. S-transform contour of the de-noised practical PD signal for α =3.

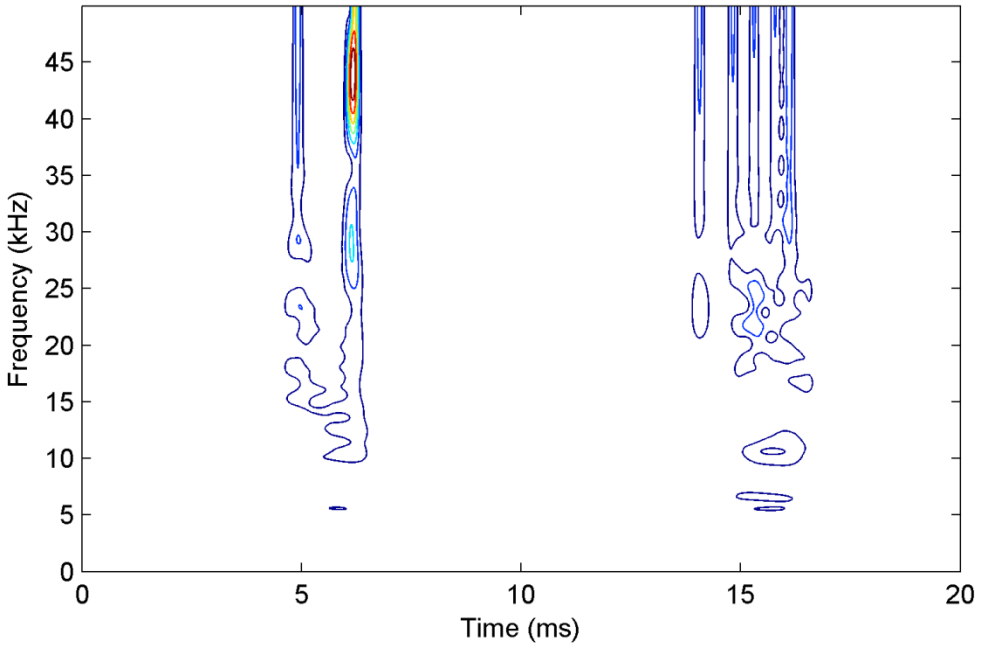

Figure 5.5. S-transform contour of the de-noised practical PD signal for α =4.

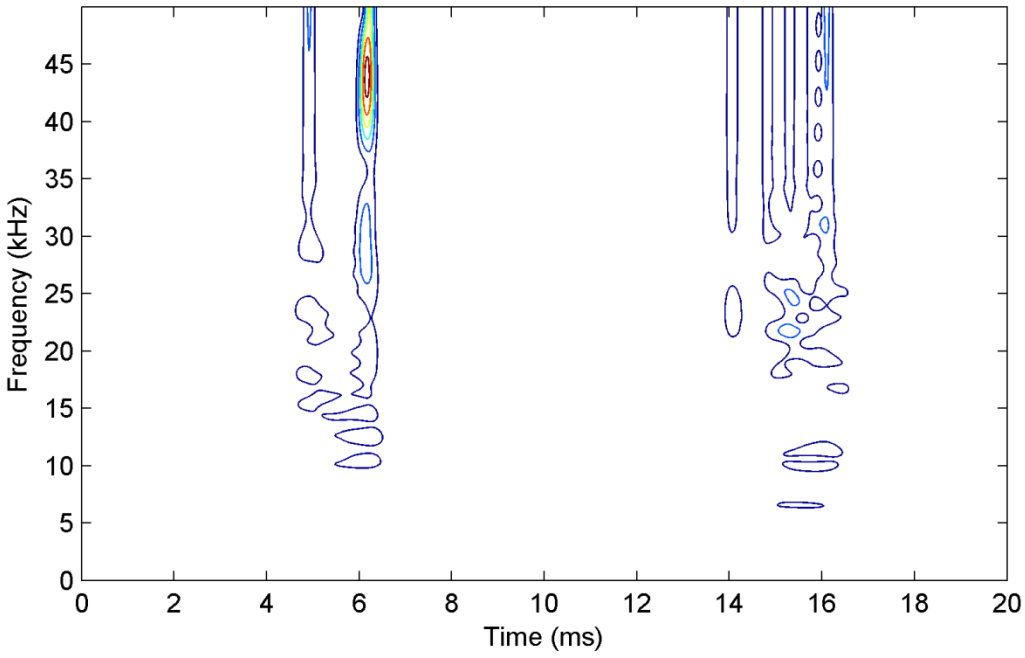

Figure 5.6. S-transform contour of the de-noised practical PD signal for α =5.

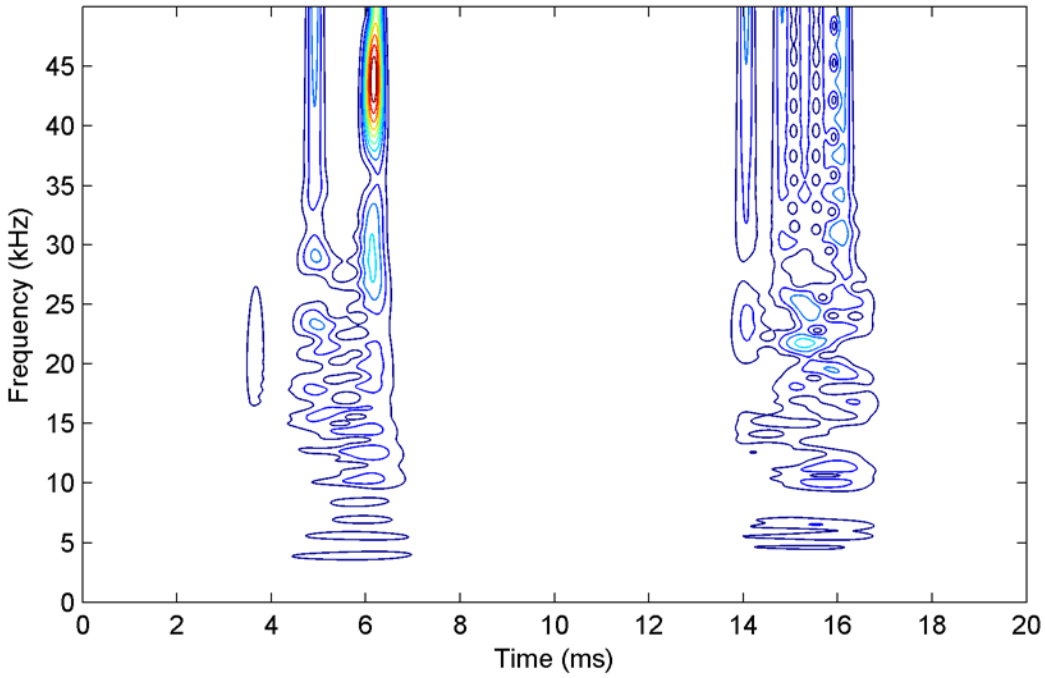

Figure 5.7. S-transform contour of the de-noised practical PD signal for α =6.

5.3 Summary

S-transform has emerged as an effective tool for time-frequency representation of a signal. In this chapter the theory of the S-transform is presented. The time-frequency representation of the noisy practical signal and de-noised practical signal are presented using S-contours of the signals. The factor α of the S-transform is varied to adjust the frequency resolution of the TFR of the signal. It is seen that as the value of the α increases, the frequency resolution of the TFR improves.

Chapter 6
Conclusion and Scope for Future Work

6.1 Conclusion

In onsite and online PD measurements, the PD signals are buried in excessive noise and interferences. Hence, the main task in the PD measurement is to extract the PD signal. Different wavelet analysis based de-noising methods are proposed in this work. Wavelet analysis is performed using DWT and SGWT where DWT is a frequency domain method and SGWT is a time domain method. Accuracy of wavelet based de-noising results depends on certain parameters like choosing proper mother wavelet, maximum decomposition level and proper thresholding rule etc. This work adopts different wavelet based de-noising techniques on five signals having different natures. Among the five signals four signals are simulated and one is a practical signal. Among the four simulated signals two are severely noised. The signals are de-noised using different DWT and SGWT based de-noising techniques. The de-noising results are compared using various evaluation parameters. It is found that the de-noising method that is most effective for a less noisy signal is not necessarily applicable to an excessively noisy signal. Again two noisy signals from different detection circuits, with same amount of noise do not adopt the same de-noising technique. For less noisy signals generally automatic thresholding rule performs better than the other options. The reconstruction based thresholding method is capable of extracting the PD signals in excessively noisy conditions. SGWT takes less time as compared to the DWT based methods in de-noising PD signals. Further, analysis of the practical PD signal is carried out using S-transform. Recently S-transform is being widely used for the time-frequency representation of a signal. Hence, S-transform is adopted for the time-frequency analysis of the practical PD signal. By varying the value of the factor α, TFR of different resolutions are obtained. It is seen that higher value of α gives better frequency resolution. Hence, the factor α plays an important role in the TFR of PD signals using S-transform.

6.2 Scope for future work

De-noising of PD signal is the main difficulty in partial discharge signal analysis. Once the signal is extracted from noise and interference, it can be studied. Wavelet analysis is a powerful tool for the partial discharge signal de-noising. Wavelet analysis of a signal can be carried out

using discrete wavelet transform and lifting wavelet transform, each of which depends on the mother wavelet chosen, maximum decomposition level chosen and the selection of thresholding rule. This work compares the different de-noising techniques applied to PD signals having different characteristics and it is seen that a more effective wavelet based de-noising technique is required which can be applied to all types of PD signals irrespective of their characteristics. An advanced automatic thresholding rule should be developed so that it works for excessively noisy signals. More research is required on lifting wavelet transform or second generation wavelet transform.

References

[1] L. Satish and B. Nazneen, “Wavelet-based denoising of partial discharge signals buried in excessive noise and interference,” IEEE Trans. Dielectrics and Electrical Insulation, vol. 10, no. 2, pp. 354-367, April 2003.

[2] X. Ma, C. Zhou and I. J. Kemp, “Interpretation of wavelet analysis and its application in partial discharge detection,” IEEE Trans. Dielectrics and Electrical Insulation, vol. 9, no. 3, pp. 446-457, June 2002.

[3] X. Zhou, C. Zhou and I. J. Kemp, “An improved methodology for application of wavelet transform to partial discharge measurement denoising,” IEEE Trans. Dielectrics and Electrical Insulation, vol. 12, no. 3, pp. 586-594, June 2005.

[4] T. S. Ramu and H. N. Nagamani, *Partial Discharge Based Condition Monitoring Of High Voltage Equipment*, New Age International (P) Ltd., Publishers, 2010.

[5] C. H. Kim and R. Aggarwal, “Wavelet transforms in power systems: Part1 General introduction to the wavelet transforms,” Power Engineering Journal, pp. 81-87, April 2000.

[6] X. Ma, C. Zhou and I. J. Kemp, “Automated wavelet selection and thresholding for PD detection,” IEEE Electrical Insulation Magazine, vol. 18, no. 2, pp. 37-45, March 2002.

[7] J. Li, T. Jiang, S. Grzybowski and C. Cheng, “Scale dependent wavelet selection for de-noising of partial discharge detection,” IEEE Trans. Dielectrics and Electrical Insulation, vol. 17, no. 6, pp. 1705-1714, Dec. 2010.

[8] H. Zhang, T. R. Blackburn, B. T. Phung and D. Sen, “A novel wavelet transform technique for on-line partial discharge measurements part 1: WT de-noising algorithm,” IEEE Trans. Dielectrics and Electrical Insulation, vol. 14, no. 1, pp. 3-14, Feb. 2007.

[9] X. Song, C. Zhou, D. M. Hepburn and G. Zhang, “Second generation wavelet transform for data denoising in PD measurement,” IEEE Trans. Dielectrics and Electrical Insulation, vol. 14, no. 6, pp. 1531-1537, Dec. 2007.

[10] R. G. Stockwell, L. Mansinha and R. P. Lowe, “Localization of the complex spectrum: The S transform,” IEEE Trans. Signal Processing, vol. 44, no. 4, pp. 998-1001, April 1996.

[11] R. G. Stockwell, “Why use the S-transform?,” American Mathematical Society, Fields Institute Communications, vol. 00, 0000.

[12] S. Mishra, C. N. Bhende and B. K. Panigrahi, “Detection and classification of power quality disturbances using S-transform and probabilistic neural network,” IEEE Trans. Power Delivery, vol. 23, no. 1, pp. 280-287, Jan. 2008.

[13] S. S. Sahu, G. Panda and N. V. George, “An improved S-transform for time-frequency analysis,” IEEE International Advance Computing Conference, Patiala, pp. 315-319, March 2009.

[14] W. Li, “Research on extraction of partial discharge signals based on wavelet analysis,” Int. Conf. on Electronic Computer Technology, pp. 545-548, Feb. 2009.

[15] M. Ben, W. J. Wei, W. J. Tong and Z. X. Mei, “MEMS gyro denoising based on second generation wavelet transform,” First Int. Conf. on Pervasive Computing, Signal Processing and Applications, pp. 255-258, Sept. 2010.

[16] M. Misiti, Y. Misiti, G. Oppenheim and J. Poggi, *Wavelet Toolbox Manual-User’s Guide*, Revised Version 4.9, The Math Works Inc., USA, 2012.

[17] P. K. Dash, B. K. Panigrahi and G. Panda, “Power quality analysis using S-transform,” IEEE Trans. Power Delivery, vol. 18, no. 2, pp. 406-411, Apr. 2003.

[18] P. K. Dash, S. R. Samantaray, G. Panda and B. K. Panigrahi, “Time–frequency transform approach for protection of parallel transmission lines,” IET Gener. Transm. Distrib., vol. 1, no. 1, pp. 30-38, Jan. 2007.

[19] A. M. Gaouda, A. El-Hag, T. K. Abdel-Galil, M. M. A. Salama and R. Bartnikas, “On-line detection and measurement of partial discharge signals in a noisy environment,” IEEE Trans. Dielectrics and Electrical Insulation, vol. 15, no. 4, pp. 1162-1173, Aug. 2008.

[20] L. Hao, P. L. Lewin, J. A. Hunter and D. J. Swaffield, “Discrimination of multiple PD sources using wavelet decomposition and principal component analysis,” IEEE Trans. Dielectrics and Electrical Insulation, vol. 18, no. 5, pp. 1702-1711, Oct. 2011.

[21] R. Polikar, *The Engineer’s Ultimate Guide to Wavelet analysis, The Wavelet Tutorial.*

[22] M. V. Chilukuri and P. K. Dash, “Multiresolution S-transform-based fuzzy recognition system for power quality events,” IEEE Trans. Power Delivery, vol. 19, no. 1, pp. 323-330, Jan 2004.

[23] H. Zhang, T. R. Blackburn, B. T. Phung and D. Sen, “A novel wavelet transform technique for on-line partial discharge measurements Part 2: on-site noise rejection application,” IEEE Trans. Dielectrics and Electrical Insulation, vol. 14, no. 1, pp. 15-22, Feb. 2007.